Article

Discovery of ARD-2051 as a Potent and Orally Efficacious Proteolysis Targeting Chimera (PROTAC) Degrader of Androgen Receptor for the Treatment of Advanced Prostate Cancer

Xin Han,[‖] Lijie Zhao,[‖] Weiguo Xiang,[‖] Bukeyan Miao,[‖] Chong Qin,[‖] Mi Wang,[‖] Tianfeng Xu, Donna McEachern, Jianfeng Lu, Yu Wang, Hoda Metwally, Chao-Yie Yang, Paul D. Kirchhoff, Lu Wang, Aleksas Matvekas, John Takyi-Williams, Bo Wen, Duxin Sun, Mark Ator, Robert Mckean, and Shaomeng Wang*
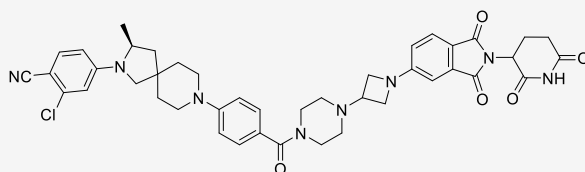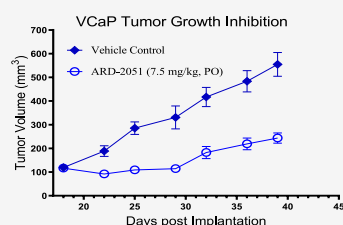
Read Online

ACCESS | Metrics & More | Article Recommendations | Supporting Information

ARD-2051 (DC$_{50}$ = 0.6 nM in VCaP and LNCaP cell)
Oral bioavailability (%): mouse/rat/dog: 53/82/46

VCaP Tumor Growth Inhibition

ABSTRACT: We report the discovery of ARD-2051 as a potent and orally efficacious androgen receptor (AR) proteolysis-targeting chimera degrader. ARD-2051 achieves DC$_{50}$ values of 0.6 nM and D_{max} >90% in inducing AR protein degradation in both the LNCaP and VCaP prostate cancer cell lines, potently and effectively suppresses AR-regulated genes, and inhibits cancer cell growth. ARD-2051 achieves a good oral bioavailability and pharmacokinetic profile in mouse, rat, and dog. A single oral dose of ARD-2051 strongly reduces AR protein and suppresses AR-regulated gene expression in the VCaP xenograft tumor tissue in mice. Oral administration of ARD-2051 effectively inhibits VCaP tumor growth and causes no signs of toxicity in mice. ARD-2051 is a promising AR degrader for advanced preclinical development for the treatment of AR+ human cancers.

INTRODUCTION

Prostate cancer (PCa) is a significant global health concern and is the second leading cause of death among men in the United States, despite the development of effective treatments.[1,2] Androgen receptor (AR), a member of the nuclear hormone receptor superfamily, is critical in the development of the prostate gland and the maintenance of male secondary sexual characteristics. Additionally, AR and AR signaling play a crucial role in the growth and development of PCa.[3,4] Androgen deprivation therapy (ADT) via either surgery or drugs blocking androgen synthesis was developed as the first-line treatment for advanced PCa.[5,6] However, patients with PCa who undergo ADT eventually develop resistance and progress to castration-resistant disease. To address this, AR antagonists have been developed for the treatment of advanced PCa, including metastatic castration-resistant PCa (mCRPC). In recent years, three second-generation AR antagonists, namely, enzalutamide (1), apalutamide (2), and darolutamide (3), have been approved for the treatment of mCRPC (Figure 1).[7−9] While these second-generation AR antagonists have improved efficacy and diminished side effects as compared to first-generation AR antagonists, resistance develops in the clinic, typically within 18 months.[10−12] However, in patients

who have acquired resistance to these second-generation AR antagonists, AR and AR signaling continue to play an important role in PCa growth and metastasis. Some of the major resistant mechanisms involving AR itself include activating point mutations, gene amplification, and expression of variants.[13−16] Therefore, AR remains an attractive therapeutic target for the development of new therapies for the treatment of mCRPC patients who have acquired resistance to these second-generation AR antagonists.[17,18]

In recent years, induced target protein degradation (TPD) using the proteolysis-targeting chimera (PROTAC) technology platform has become an exciting new therapeutic strategy. Structurally, PROTACs are hetero-bifunctional small-molecules consisting of a ligand binding to a target protein of interest (POI), a second ligand binding to an E3 ligase or an E3 ligase complex, tethered together through a linker. A
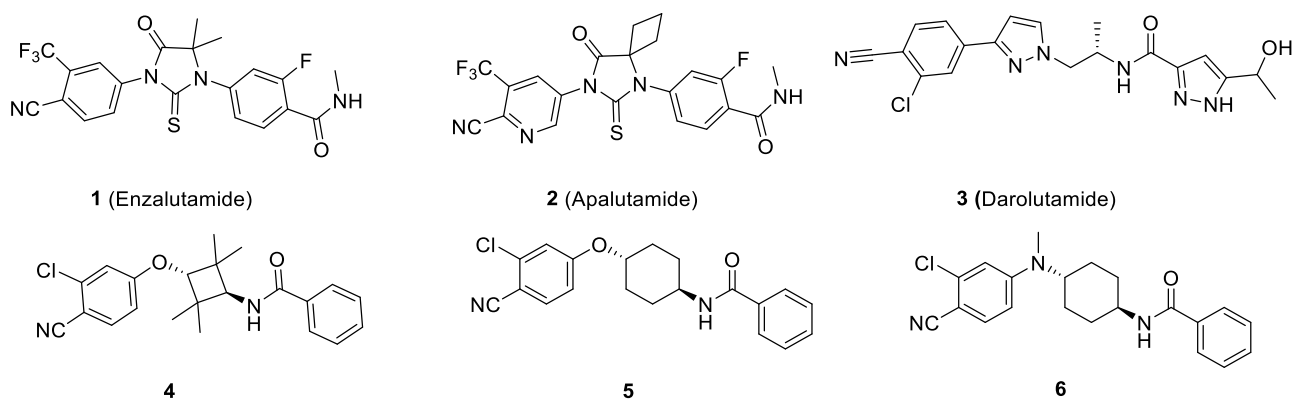
Figure 1. Chemical structures of representative AR antagonists and ligands.
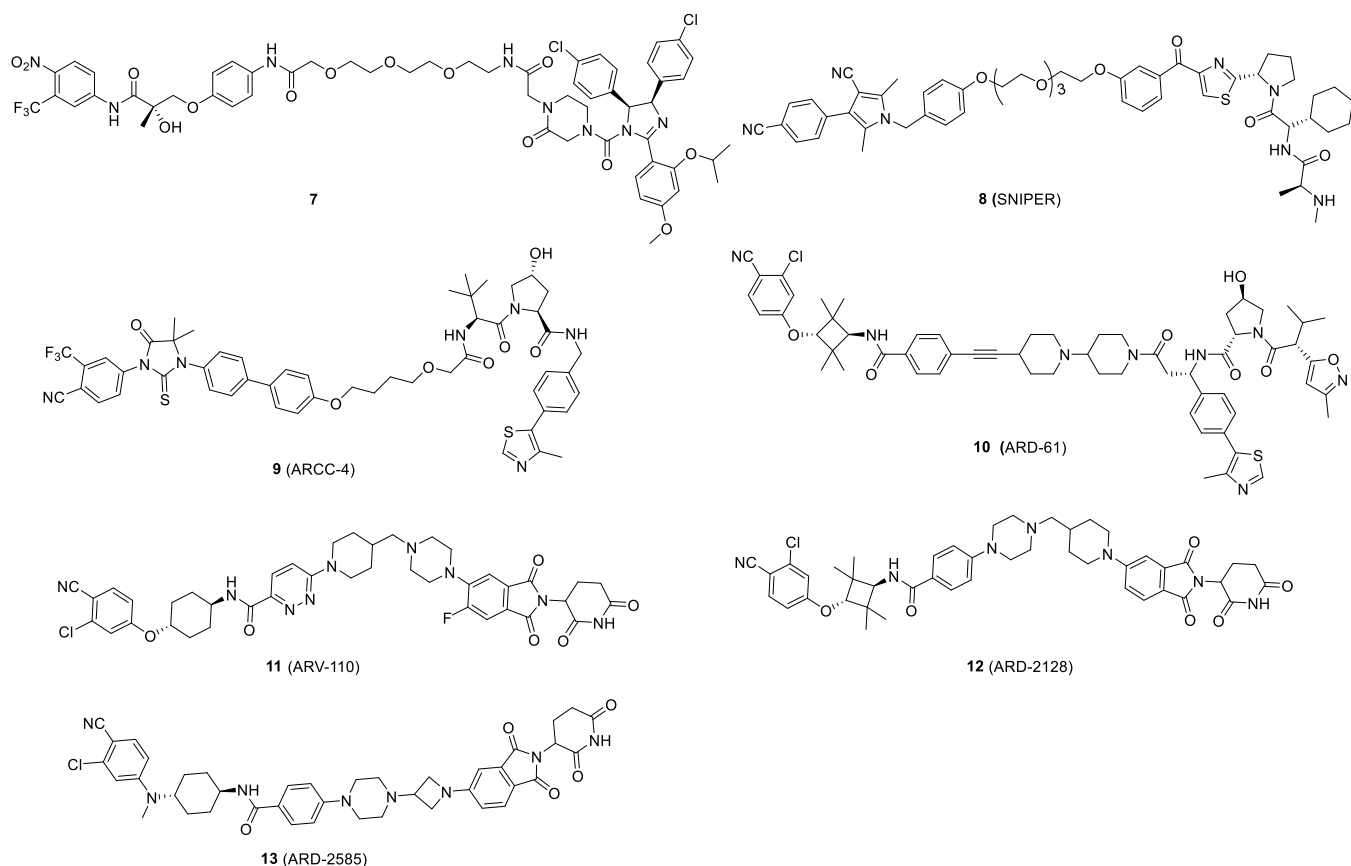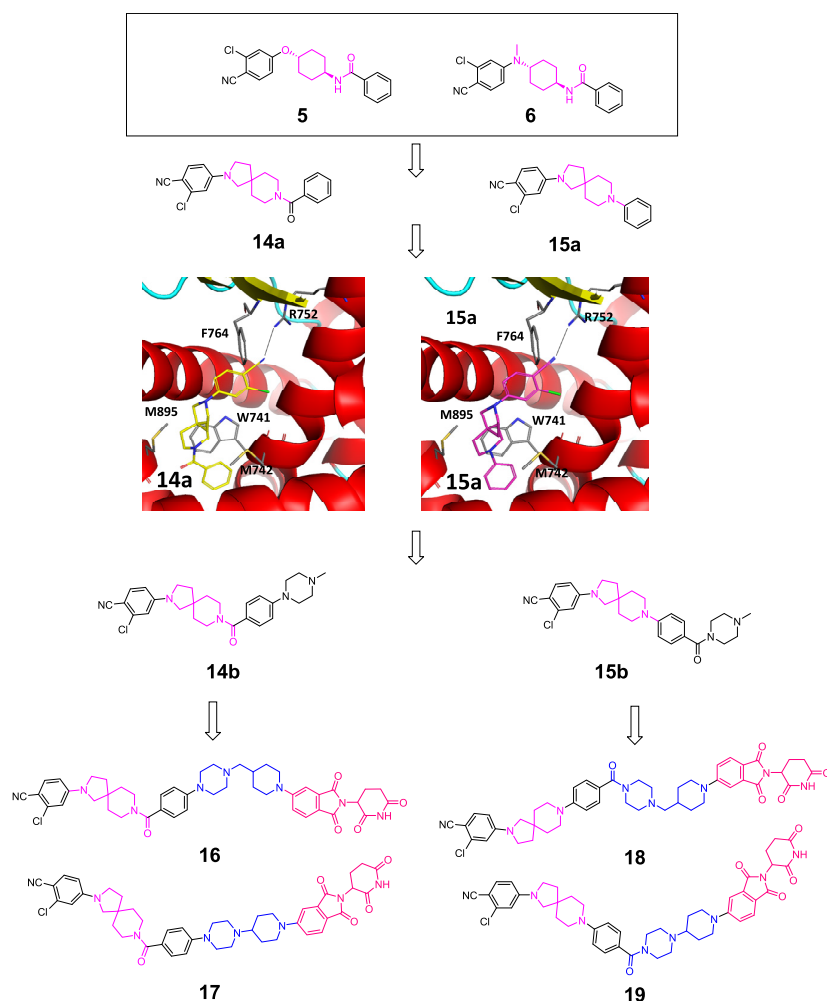

Figure 2. Chemical structures of representative PROTAC AR degraders.

PROTAC degrader recruits the POI to an E3 ligase or an E3 ligase complex for ubiquitination, followed by proteosome-dependent degradation of the POI.[19,20] In the last few years, PROTAC AR degraders have been designed using different classes of AR ligands and ligands for 4 classes of E3 ligases, namely, MDM2, IAPs, VHL/cullin 2, and cereblon/cullin 4A (Figure 2).[21−30] While PROTAC AR degraders designed using ligands for MDM2 and IAP proteins are not very potent, highly potent PROTAC AR degraders using ligands for VHL and cereblon have been discovered. Because PROTAC degraders typically have MW greater than 700, achieving oral bioavailability has been a major challenge.[31] However, through extensive medicinal chemistry efforts, a number of potent and orally active AR degraders have been reported, as represented by ARV-110, ARD-2128, and ARD-2585 (Figure 2) using a

cereblon ligand.[32−40] Importantly, several orally active AR degraders, including ARV-110, have been advanced into clinical development.[18] Early clinical data showed that ARV-110 has a good safety profile and demonstrates clinical activity in patients heavily treated with second-generation AR antagonists or abiraterone, particularly for those patients carrying AR T878 and/or H875 mutations.[32] The encouraging early clinical data on ARV-110 suggest that orally active AR degraders have the potential to be developed as a new class of therapies for the treatment of advanced PCa, including mCRPC.

In the present study, we report our design, synthesis, and characterization of a new class of PROTAC AR degraders. Our efforts led to the discovery of ARD-2051 as a highly potent and

Figure 3. Design of a new class of AR ligands and PROTAC degraders, predicted binding models for ligands **14a** and **15a** in complex with human AR in its agonist conformation and summary of AR degradation data in AR + VCaP cells. VCaP cells were treated with designed PROTAC degraders for 24 h for Western blotting analysis for AR protein levels.

No.	Compound	% AR protein degradation in VCaP cells (μM)		
		0.01	0.1	1
16	ARD-1551	<5	<5	33
17	ARD-1048	<5	43	56
18	ARD-1093	24	80	>95
19	ARD-1120	24	74	95

orally efficacious AR degrader suitable for advanced preclinical development.

■ RESULTS AND DISCUSSION

We have previously employed AR ligand **6** for the design of a highly potent and orally active PROTAC AR degrader ARD-

2585.[34] While ARD-2585 has an oral bioavailability of 51% in mice, it only has a moderate oral bioavailability of 13% in rats. We therefore sought to design new and potent PROTAC degraders with excellent oral bioavailability not only in mice but also in other species for the purpose of clinical development.

We hypothesized that new AR ligands with a reduced polar surface as compared to that for AR ligand **6** could provide us with an opportunity to design PROTAC AR degraders with good oral bioavailability across animal species.

In our previous study, we predicted the binding models of AR ligand **6** in complex with AR.[33,34] Analysis of our modeled structures suggested that the chemical moiety linking the two phenyl groups in AR ligand **6** have hydrophobic contacts with AR but lack hydrogen bonding or polar interactions with AR. Therefore, we proposed compounds **14a** and **15a** as potential new AR ligands. Modeling showed that compounds **14a** and **15a** bind to AR with similar overall binding modes (Figure 3 and Supporting Information, SI). Specifically, the nitrile group in both compounds forms a strong hydrogen bond with the side chain of Arg752 and the Cl group inserts into a hydrophobic cavity formed by Met745, Met749 and Met787. The terminal phenyl group in both compounds adopts a conformation to achieve $\pi-\pi$ stacking with Trp741, similar to what was observed in the predicted binding model for AR ligand **6**.

We synthesized **14a** and **15a** and evaluated their binding to AR using a fluorescence-polarization (FP) assay, with enzalutamide included as a control. Our binding data showed that compound **14a** has an IC_{50} value of 1.7 μM, whereas **15a** has an IC_{50} value of >1 μM (IC_{50} = 30% at 1 μM). In comparison, enzalutamide has an IC_{50} value of 0.8 μM in the same assay.

For the design of AR PROTAC degraders, a tethering site is needed. In our previous potent and orally active AR degraders ARD-2585 and ARD-2128, we employed a piperazine appended onto the AR ligands to tether to a cereblon ligand through a linker. We therefore designed and synthesized compound **14b** by installing a 1-methyl-4-phenylpiperazine group onto the phenyl ring in **14a**. Compound **14b** binds to AR with IC_{50} values of 0.8 μM, thus being 2 times more potent than **14a**. For compound **15a**, we inserted an additional carbonyl group between the phenyl ring and 1-methyl-4-phenylpiperazine group to enhance the chemical and metabolic stability, which resulted in compound **15b**. Surprisingly but gratifyingly, compound **15b** binds to AR with an IC_{50} value of 78 nM, representing a very potent AR ligand.

Using **14b** and **15b** as AR ligands, we designed and synthesized 4 potential PROTAC AR degraders **16−19** using those optimal linkers we identified from our previous studies and thalidomide as the cereblon ligand.[33,34]

We evaluated these four potential AR degraders for their AR degradation in the AR + VCaP cell line with the data summarized in Figure 3. While compound **16** has a minimal effect on the levels of AR protein at concentrations of 10, 100 and 1000 nM, compound **17** reduces the AR protein by <5, 43, and 56% at 10 nM, 100 nM, and 1 μM, respectively. In comparison, compounds **18** and **19** are more effective than compound **17** at both 100 nM and 1 μM in reducing the levels of AR protein, achieving >70% of AR degradation at 100 nM and >90% AR degradation at 1 μM for both compounds. Hence, compounds **18** and **19** represented two reasonably potent AR degraders for further optimization.

Our previous studies showed that the linker in an AR PROTAC degrader plays a critical role for its degradation potency and pharmacokinetics (PKs).[18,33,34] We next performed further modifications of the linkers in compounds **18** and **19**. Our previous studies[33,34] have also suggested that positively charged and conformationally constrained linkers are

preferred to achieve potent AR degradation and oral bioavailability.[33,34] Accordingly, we have synthesized a series of analogues of compounds **18** and **19** by employing a conformationally constrained linker containing a positively charged amine group and evaluated them for their AR degradation in the VCaP cell line with the data summarized in Table 1.

Table 1. Optimization of Rigid Linkers Based Upon Compound 19
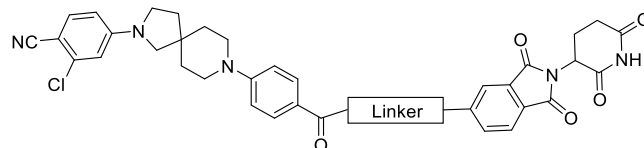
No.	Compound	Linker	% AR protein degradation in VCaP Cells (μM)		
			0.01	0.1	1
18	ARD-1093		24	80	>95
19	ARD-1120		24	74	95
20	ARD-1152		37	20	>95
21	ARD-1137		45	80	92
22	ARD-1119		<5	54	54
23	ARD-1115		23	80	90
24	ARD-1138		<5	46	73
25	ARD-1118		20	60	82
26	ARD-1149		30	81	85
27	ARD-1140		78	>95	>95
28	ARD-2007		39	70	87
29	ARD-1184		22	62	81

Compound **20** was synthesized by swapping the piperidine and piperazine groups in the linker of compound **19**. While **20** achieves >95% of AR degradation at 1 μM, it is less effective in reducing the AR protein level at 100 nM than **19**. Expanding the ring size from the 6-membered piperazine in **19** to a 7-membered, 1,4-diazepane led to compound **21**, which has a similar degradation potency as compared to **19**. Expanding the 7-membered, 1,4-diazepane ring in **21** to an 8-membered, 1,4-diazepane ring generated compound **22**, which is weaker in inducing AR degradation than compound **21**. Constraining the

8-membered, 1,4-diazepane ring in **22** resulted in compound **23**, which is more potent than **22** but slightly less potent than **21**. Replacing the mono-cyclic piperazine group in **19** with a bicyclic 2,6-diazaspiro[3.3]heptane ring yielded compound **24**, which is less potent than **19** in AR degradation. Changing the [4,4] spiro-ring in **24** with a [5,4] spiro-ring generated **25**, which is more potent than **24** but still less potent than **19**. Replacing the piperidine in **19** with 3-methylazetidine led to compound **26**, which has a similar AR degradation potency as compared to **19**.

Removing the methylene group in the linker in compound **26** resulted in **27**, which is a potent AR degrader. Compound **27** reduces the levels of AR protein by 78, >95, and >95% at 10, 100 nM, and 1 μM, respectively, and is thus more potent than **19**. Replacing the 6-membered piperazine group in **27** with a 7-membered, 1,4-diazepane ring yielded compound **28**, which is less potent than **27**. Similarly, replacing the 6-membered piperazine group in **27** with a bicyclic 2,6-diazaspiro[3.3]heptane ring generated compound **28**, which is also less potent than **27**. Hence, our linker modifications of compounds **18** and **19** led to the identification of compound **27** as a potent AR degrader.

We assessed oral plasma exposure for compounds **20**, **21**, and **27** in mice with a single oral administration at 10 mg/kg with the data summarized in Table 2. Although compounds **20**

Table 2. Assessment of Oral Exposure of Compounds 20, 21, and 27 in Mice[a]

	plasma drug concentration (mean ± SD, ng/mL)			
compound	1 h	3 h	6 h	24 h
20 (ARD-1152)	82[b]	57[b]	91[b]	3[b]
21 (ARD-1137)	46 ± 16	8 ± 1	11 ± 3	NA
27 (ARD-1140)	501 ± 106	171 ± 83	246 ± 27	44 ± 5

[a]Each compound was administered with a single dose at 10 mg/kg via oral gavage using 100% PEG200 as the formulation. [b]Mean plasma drug concentrations from two mice at each time-point. For compounds **21** and **27**, 3 mice were used for each compound for each time-point.

and **21** have modest oral plasma exposure, compound **27** achieves good oral exposure with plasma concentrations of 501, 171, 246, and 44 ng/mL at 1, 3, 6, and 24 h time-points, respectively.
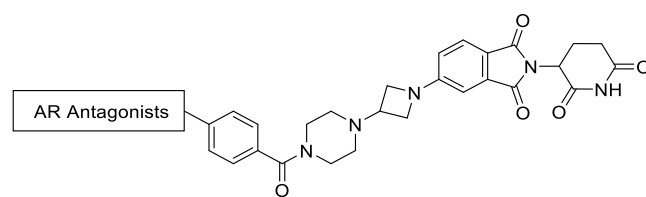
Hence, compound **27** is a potent AR degrader with a DC_{50} value of <10 nM and a D_{max} of >95% and achieves good oral exposure in mice. We next performed further modifications of the AR antagonist portion in compound **27**.
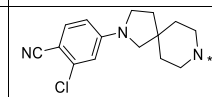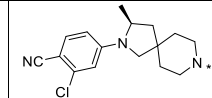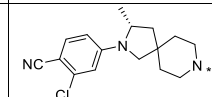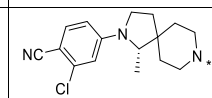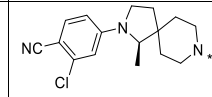
Our predicted binding model for AR ligand **15a** (Supporting Information) showed that there is additional room available around the [6,5] spiro ring. Accordingly, we introduced a methyl group in two different positions of the five-membered ring with the objective to enhance AR degradation potency.

We synthesized compounds **30** and **31** by introducing a chiral methyl group onto 3-position of the spiro ring. Compound **30** (ARD-2051) with *S*-methyl group is highly potent AR degrader and more potent than compound **31** with *R*-methyl group (Figure 3). In fact, ARD-2051 reduces the levels of AR protein by >95% at 10, 100, and 1000 nM (Table 3).

We synthesized compounds **32** and **33** with a chiral methyl group onto 1-position of the spiro ring. Compound **32** with 1-*S*-methyl substitution is a potent AR degrader, capable of

Table 3. Optimization of AR Antagonist Portion in Our AR Degraders

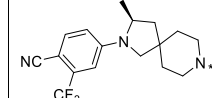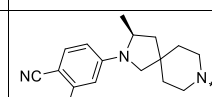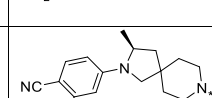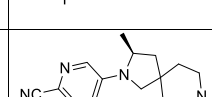| No.	Compound	AR Antagonists	% AR protein degradation in VCaP Cells (µM)		
			0.01	0.1	1
27	ARD-1140		78	>95	>95
30	ARD-2051		>95	>95	>95
31	ARD-2052		66	93	>95
32	ARD-2061		84	>95	>95
33	ARD-2062		46	68	91
34	ARD-2075		>90	>95	>95
35	ARD-2076		>90	>95	>95
36	ARD-2094		>90	>95	>95
37	ARD-2065		>90	>95	>95

reducing the AR protein level by 84% at 10 nM and >95% at 100 and 1000 nM. Compound **33** with 1-*R*-methyl substitution is still a reasonably potent AR degrader but is much less potent than compound **32**.

Based upon our predicted binding model (Supporting Information) for AR ligands **15a**, the nitrile group forms a strong hydrogen bond with the side chain of Arg752 and the Cl group inserts into a hydrophobic cavity formed by Met745, Met749, and Met787. We replaced the Cl substitution on the phenyl ring in compound **30** with CF_3, CF_2H, or F
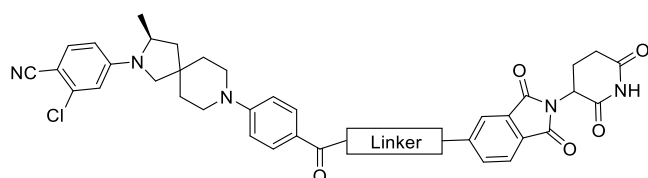
substitution, respectively, which yielded compounds **34**, **35**, and **36**, respectively. Compounds **34−36** are all potent and effective AR degraders, capable of reducing AR protein by >90% at 10 nM and >95% at 100 nM and 1000 nM.

We inserted a nitrogen into the substituted phenyl ring in compound **34** to improve its solubility, which led to compound **37**. Compound **37** reduces the levels of AR protein >90% at 10 nM and >95% at 100 nM and 1000 nM and is therefore a very potent and effective AR degrader.

We next designed and synthesized a series of new analogues of ARD-2051 by employing a series of conformationally constrained linkers with lengths similar to that in ARD-2051, and the results are summarized in Table 4.

Among these new analogues, **38** (ARD-2509), **39** (ARD-1669), **43** (ARD-2378), **44** (ARD-2070), and **48** (ARD-2067) are capable of reducing the AR protein levels by >90% at 10

nM and achieve D_{max} values of >95%. In comparison, compounds **40**, **41**, **42**, and **46** are less potent AR degraders than ARD-2051.

Assessment of Oral Exposures of Potent AR Degraders in Mice. We evaluated a number of highly potent compounds for their oral exposures in mice with ARV-110 included as the control with the data summarized in Table 5.

Table 5. Assessment of Oral Exposure of Several Highly Potent AR Degraders in Mice[a]

compound	plasma drug concentration (mean ± SD, ng/mL)			
	1 h	3 h	6 h	24 h
30 (ARD-2051)	495 ± 49	664 ± 87	369 ± 73	77 ± 9
34 (ARD-2075)	31 ± 4	56 ± 10	29 ± 7	BLQ
36 (ARD-2094)	134 ± 52	146 ± 37	91 ± 17	BLQ
37 (ARD-2065)	571 ± 205	678 ± 199	451 ± 161	BLQ
39 (ARD-1669)	238 ± 55	208 ± 36	104 ± 25	BLQ
ARV-110	55 ± 15	124 ± 23	110 ± 12	70 ± 9

[a]Each compound was administered via oral gavage at 10 mg/kg and mice were sacrificed at indicated time-points and each time-point used 3 mice for each compound. BLQ: below the level of quantification.

The oral exposure data showed that ARD-2051 and ARD-2065 have excellent oral plasma exposures in mice, whereas ARD-1669 and ARD-2094 has good oral exposure and ARD-2075 has a modest oral exposure. In direct comparison, ARD-2051 has better oral plasma exposure than ARV-110, as evident by the higher plasma drug concentrations at 1, 3, and 6 h time-points and a similar drug concentration at 24 h time-point for ARD-2051 and ARV-110. Based upon the oral exposure data in mice, ARD-2051 was selected for further evaluation.

Further Evaluation of ARD-2051 in AR+ Prostate Cancer Cell Lines. We next evaluated ARD-2051 in more details for its degradation potencies and cell growth inhibition in the VCaP and LNCaP cell lines. We included ARV-110, which is currently in phase I/II clinical trials as a positive control in these experiments. The data are summarized in Table 6.

ARD-2051 achieves a DC_{50} value of 0.6 nM in both the VCaP and LNCaP cell lines and D_{max} of 97 and 92% in the VCaP and LNCaP cell lines, respectively. In comparison, ARV-110 attains DC_{50} values of 3.6 and 5.5 nM in the VCaP and LNCaP cell lines, respectively, and D_{max} of 92 and 81% in the VCaP and LNCaP cell lines, respectively. Hence, ARD-2051 is 6−9 times more potent than ARV-110 in inducing AR degradation in the VCaP and LNCaP cell lines. Furthermore, ARD-2051 also demonstrates better D_{max} than ARV-110 in these two AR+ cell lines.

In the cell growth inhibition assay, ARD-2051 has an IC_{50} value of 10.2 and 12.8 nM in the VCaP and LNCaP cell lines, respectively, and I_{max} of 98 and 100% in the VCaP and LNCaP cell lines, respectively. In comparison, ARV-110 demonstrates IC_{50} values of 41.3 and 32.1 nM in the VCaP and LNCaP cell lines, respectively, and I_{max} of 88 and 90% in the VCaP and LNCaP cell lines, respectively. Thus, consistent with the degradation data, ARD-2051 is more potent and achieves better I_{max} than ARV-110 in cell growth inhibition in both the VCaP and LNCaP cell lines.

We investigated the mechanism of AR degradation induced by ARD-2051. Our data showed that AR degradation induced by ARD-2051 is effectively blocked by an AR antagonist (ARi-

Table 4. Further Modifications of the Linker Portion Based Upon ARD-2051

No.	Compound	AR antagonist portion	% AR protein degradation in VCaP Cells (μM)		
			0.01	0.1	1
30	ARD-2051		>90	>95	>95
38	ARD-2509		>90	>95	>95
39	ARD-1669		>90	>95	>95
40	ARD-7001		81	>95	>95
41	ARD-7002		78	>95	>95
42	ARD-2063		79	>95	>95
43	ARD-2378		>90	>95	>95
44	ARD-2070		>90	>95	>95
45	ARD-2071		84	93	95
46	ARD-2090		12	64	92
47	ARD-2091		81	93	88
48	ARD-2067		>90	>95	>95

Table 6. AR Degradation and Cell Growth Inhibition of ARD-2051 and ARV-110 in AR+ VCaP and LNCaP Cell Lines[a]

	VCaP cell line				LNCaP cell line			
	AR degradation		cell growth inhibition		AR degradation		cell growth inhibition	
	DC_{50} (nM)	D_{max} (%)	IC_{50} (nM)	I_{max} (%)	DC_{50} (nM)	D_{max} (%)	IC_{50} (nM)	I_{max} (%)
ARV-110	3.6 ± 0.7	92 ± 1	41 ± 16	88 ± 3	5.5 ± 2.8	81 ± 6	32 ± 8	90 ± 2
ARD-2051	0.6 ± 0.1	97 ± 1	10 ± 3	98 ± 3	0.6 ± 0.1	92 ± 2	13 ± 1	100 ± 3

[a]For AR degradation, cells were treated for 24 h for Western blotting analysis with actin used as the loading control. For cell growth inhibition, cells were treated for 4 days and cell viability was determined by an WST-8 assay.

12), a cereblon ligand (thalidomide), a proteasome inhibitor (MG132), and a NEDD8 inhibitor (MLN4924) in the VCaP and LNCaP cell lines (Figure 4). These data demonstrate that ARD-2051 is a bona fide PROTAC AR degrader.
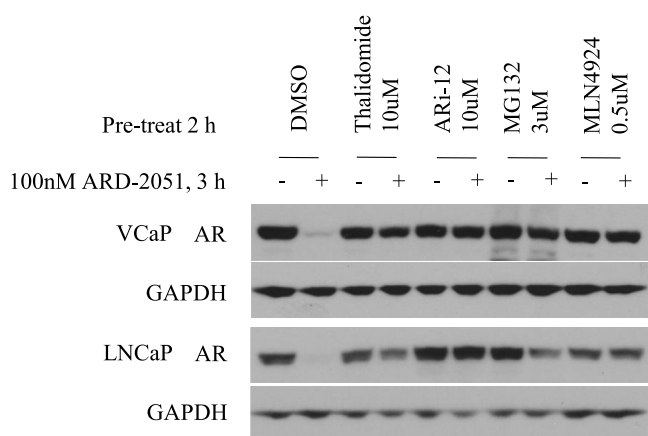

Figure 4. Evaluation of the mechanism of action of ARD-2051. VCaP and LNCaP cells were pretreated for 2 h with DMSO, an AR inhibitor ARi-12 (10 μM), thalidomide (10 μM), a proteasome inhibitor MG-132 (3 μM), and an E1 neddylation inhibitor MLN4924 (0.5 μM). Cells were then treated for 3 h with ARD-2051 at 100 nM. Total protein was analyzed by Western blotting. GAPDH was used as the loading control.

We investigated the ability of ARD-2051 to suppress the expression of *KLK3* (PSA), a key gene regulated by AR protein in both LNCaP and VCaP cell lines, with enzalutamide, an AR antagonist, included as the control. The data are summarized in Figure 5.

Our quantitative real-time polymerase chain reaction (qRT-PCR) data (Figure 5) showed that ARD-2051 effectively and potently suppresses the expression of *KLK3* gene in both LNCaP and VCaP cell lines in a dose-dependent manner. In the LNCaP cell line, ARD-2051 suppresses the expression of *KLK3* gene by 53% at 0.3 nM and is equally effective as enzalutamide at 100 nM. ARD-2051 at 10 nM suppresses the expression of *KLK3* gene by 79% and is as effective as enzalutamide at 1000 nM. In the VCaP cell line, ARD-2051 suppresses the expression of *KLK3* gene by 51% at 1 nM and by 87% at 30 nM, respectively. In comparison, ARD-2051 at 30 nM is as effective as enzalutamide at 1000 nM in the VCaP cell line. Hence, ARD-2051 is at least 30 times more potent than enzalutamide in suppressing the expression of *KLK3* gene in VCaP and LNCaP cell lines.

Proteomic Analysis of Degradation Selectivity for ARD-2051 in VCaP Cells. We performed a proteomic analysis to assess the degradation selectivity of ARD-2051 in the VCaP cell line with its corresponding AR ligand ARi-12 included as the control. VCaP cells were treated with ARD-2051 at 100 nM or 1 μM, or with ARi-12 at 10 μM for 24 h time-point for multiplexed quantitative proteomics analysis. The data are summarized in Figure 6.
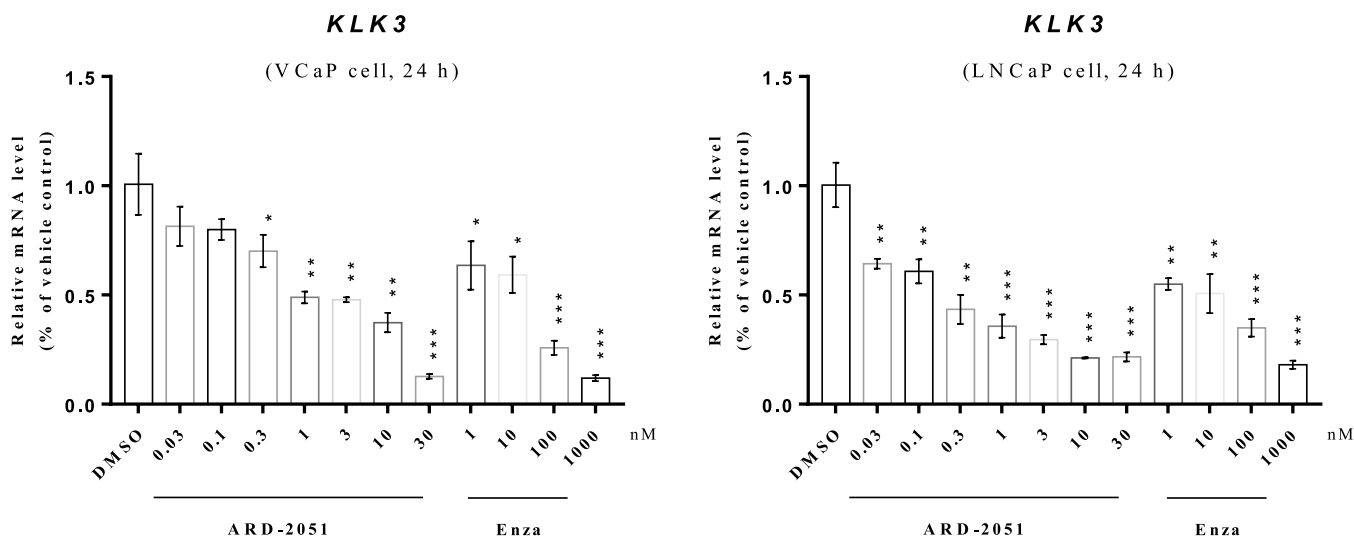

Figure 5. Suppression of the *KLK3* (PSA) gene by ARD-2051 and enzalutamide in the AR+ LNCaP and VCaP cell lines. VCaP and LNCaP cells were treated for 24 h, and qRT-PCR was performed to determine the mRNA levels for *KLK3* gene. *, $0.01 \leq p < 0.05$; **, $0.001 \leq p < 0.01$; ***, $p < 0.001$.
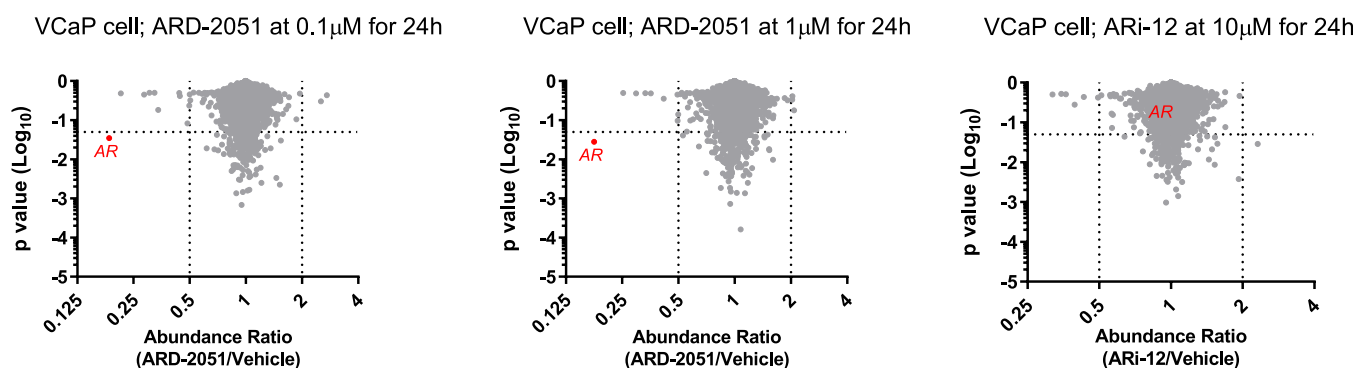
Figure 6. Multiplexed quantitative proteomics analysis of ARD-2051 and its corresponding inhibitor ARi-12 in VCaP cells. VCaP cells were treated with ARD-2051 at 100 nM or 1 μM, or ARi-12 at 10 μM for 24 h for proteomic analysis. Relative abundance of protein levels was normalized to DMSO-treated cells. Each experiment was performed in three independent replicates. Proteins with p value ≤ 0.05 (y axis) and fold changes greater than 2 (x axis) are colored in red.

ARD-2051 at both 100 nM and 1 μM effectively and profoundly reduced the levels of AR protein by 82% ($p < 0.05$). Importantly, among >5700 proteins analyzed, AR was the only protein whose levels were significantly reduced by more than 2-fold by ARD-2051. ARD-2051 did not induce upregulation of any proteins significantly. In comparison, the corresponding inhibitor ARi-12 did not significantly alter the levels of any proteins analyzed. Taken together, our data showed that ARD-2051 is a potent and selective degrader of AR protein.

Evaluation of ARD-2051 for Its Liver Microsomal Stability, Hepatocyte Stability, Plasma Stability, and Plasma Protein Binding, CYP Inhibition and hERG Inhibition. We evaluated ARD-2051 for its liver microsomal stability, hepatocyte stability, plasma stability, and plasma protein binding in mouse, rat, dog, monkey and human, and the data are summarized in Table 7.

Table 7. Liver Microsome Metabolic Stability, Hepatocyte Stability, Plasma Stability, and Plasma Protein Binding of ARD-2051 in Five Species (Human, Mouse, Rat, Dog, and Monkey)

species	$T_{1/2}$ (min)			plasma protein binding (%)
	liver microsomal stability	hepatocyte stability	plasma stability	
mouse	>60	>120	>120	99.2
rat	>60	>120	>120	99.1
dog	>60	>120	>120	99.3
monkey	>60	>120	>120	99.2
human	>60	>120	>120	99.1

Our data indicate that ARD-2051 exhibits exceptional stability in liver microsomes, hepatocytes, and plasma across all five species studied. ARD-2051 displays a high level of plasma protein binding, ranging from 99.1 to 99.3%, across mouse, rat, dog, monkey, and human species (Table 7). These findings demonstrate that ARD-2051 has a similar high plasma protein binding profile with a detectable level of free drug fraction in plasma across all five species.

ARD-2051 was evaluated for its cytochrome P450 (CYP) inhibitory activity against 7 major CYP isoforms. ARD-2051 has no significant effect on CYP inhibition up to 10 μM (Table 8).

Table 8. CYP Inhibition and hREG Inhibition of ARD-2051

CYP inhibition (IC$_{50}$, μM)								hERG inhibition (IC$_{50}$, μM)
1A2	2B6	2C8	2C9	2C19	2D6	3A4 (M)	3A4 (T)	
>10	>10	>10	>10	>10	>10	>10	>10	>30

ARD-2051 was tested for its potential hERG inhibition and shown to have no significant hERG inhibition up to 30 μM (Table 8).

Pharmacokinetic Studies of AR-2051 in Mouse, Rat, and Dog. Toward our goal of identifying a promising AR degrader for clinical development, we evaluated the PK of ARD-2051 in mouse, rat, and dog with both intravenous (IV) and oral administration, obtaining the data summarized in Table 9.

In the mouse, ARD-2051 has an excellent overall PK profile, with a low clearance (Cl = 3.7 mL/min/kg), a moderate volume of distribution (V_{ss} = 1.3 L/kg), a half-life of approximately 5 h with both IV and oral routes of administration, and an excellent oral exposure with a good oral bioavailability (F) of 53%.

In the rat, ARD-2051 has a low-moderate clearance (Cl = 10.2 mL/min/kg), a moderate volume of distribution (V_{ss} = 1.3 L/kg), a half-life of 2−2.3 h with intravenous (IV) and oral routes of administration, and an excellent oral bioavailability (F) of 82%.

In the dog, ARD-2051 has a low-moderate clearance (Cl = 4.6 mL/min/kg), a good volume of distribution (V_{ss} = 2.8 L/kg), a long half-life of 8.9 h with the IV route of administration and 21.1 h with oral route of administration, an excellent oral exposure (C_{max} = 294 ng/mL and AUC = 1822 h*mg/mL at 1 mg/kg), and an oral bioavailability (F) of 46%.

Taken together, these data show that ARD-2051 has a good overall PK profile in the mouse, rat, and dog with excellent oral bioavailability.

Pharmacodynamic Evaluation of ARD-2051 in VCaP Xenograft Tumors. Based upon its promising PK profile in mice and excellent potencies in AR degradation, we evaluated the ability of ARD-2051 in reducing AR protein levels in VCaP xenograft tumors in mice through a pharmacodynamic (PD) study.

Our Western blotting data (Figure 7A,B) showed that a single oral administration of ARD-2051 at 12.5 mg/kg

Table 9. Summary of PK Data for ARD-2051 in Mouse, Rat, and Dog[a]

	route	dose (mg/kg)	$T_{1/2}$ (h)	AUC_{0-t} (h*mg/mL)	Cl (mL/min/kg)	V_{ss} (L/kg)	route	dose	$T_{1/2}$ (h)	C_{max} (mg/mL)	AUC_{0-t} (h*mg/mL)	F (%)
male ICD mouse	IV[b]	2	5	8846	3.7	1.3	PO[b]	5	4.9	1476	11684	53
male SD rat	IV[b]	1	2.1	1563	10.2	1.3	PO[c]	10	3.9	1473	12781	82
male beagle dog	IV[b]	1	8.9	3235	4.6	2.8	PO[d]	3	3.4	294	4464	46

[a]C_{max}, maximum drug concentration; AUC_{0-24h}, area under the curve between 0 and 24 h; Cl = plasma clearance rate; V_{ss} = steady state volume of distribution; $T_{1/2}$ = terminal half-life, F = oral bioavailability; IV, intravenous administration. [b]Vehicle: 10% PEG400 + 90% PBS (pH 8). [c]Vehicle: 5% DMSO +10% solutol + 85% saline. [d]90% PEG400 + 10% cremophor.
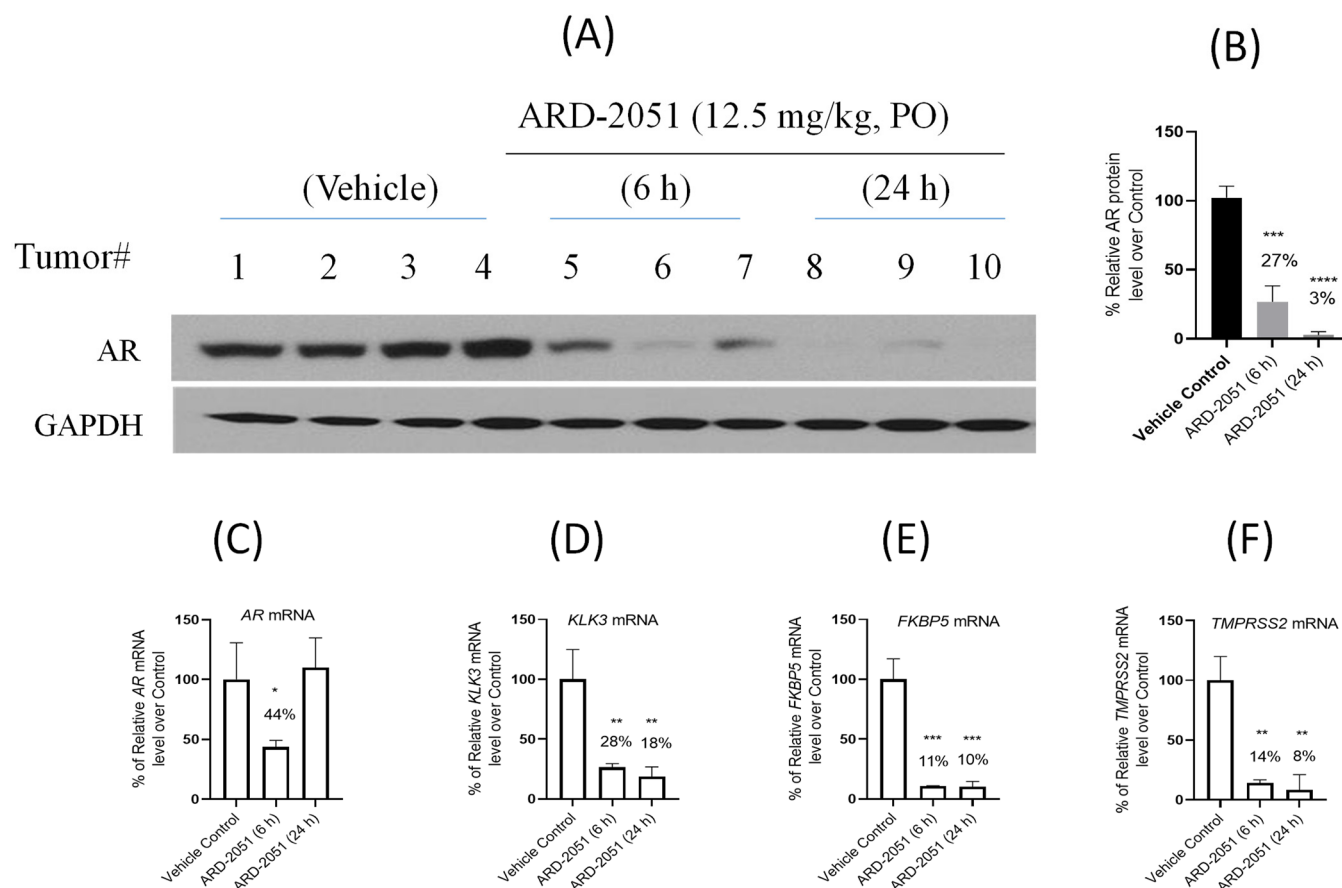

Figure 7. Pharmacodynamic analysis of ARD-2051 in the VCaP xenograft model in SCID mice. SCID mice bearing VCaP tumors were treated with a single oral administration of ARD-2051 at 12.5 mg/kg. Mice were euthanized at indicated time-points for collection of plasma and tumor tissues for analysis. (A) Western blotting analysis of AR protein in VCaP tumors. (B) Quantification of AR protein levels of the Western blots. (C−F) qRT-PCR analysis of mRNA levels of *AR*, *KLK3*, *FKBP5*, and *TMPRSS2* in VCaP tumor tissue. *, $0.01 \leq p < 0.05$; **, $0.001 \leq p$ 0.01; ***, $0.0001 \leq p$ 0.001; ****, $0.00001 \leq p$ 0.0001.

effectively reduces the levels of AR protein in the VCaP tumor tissue in mice. ARD-2051 reduces the AR protein levels by 73% at 6 h time-point and by >95% at the 24 h time-point.

We performed qRT-PCR analysis on the tumor tissues to determine the mRNA levels of three AR-regulated genes. Our data (Figure 7D−F) showed that ARD-2051 effectively reduces the mRNA levels of *KLK3* (encoding PSA), *FKBP5*, and *TMPRSS2* genes at both 6 and 24 h time points. Interestingly, ARD-2051 has a significant effect ($p = 0.04$) in reducing the mRNA levels of *AR* gene at 6 h time-point but not at the 24 h time-point.

To gain further insights into the PD data, we determined the drug concentrations in both plasma and tumor tissue for ARD-2051 with obtained data summarized in Table 10. ARD-2051

Table 10. Determination of Drug Concentrations in Plasma and VCaP Tumor Tissue in SCID Mice for ARD-2051[a]

compound	time-point (h)	plasma concentration (ng/mL) mean ± SD	tumor concentration (ng/mL) mean ± SD
ARD-2051	6	985 ± 903	946 ± 341
	24	742 ± 234	183 ± 131

[a]ARD-2051 was administered with a single PO dose at 12.5 mg/kg with 100% PEG200 as the formulation in mice bearing VCaP tumors with one tumor per mouse. Plasma and tumor tissue were collected at 6 and 24 h time-points for ARD-2051 with 3 mice for each time-point.
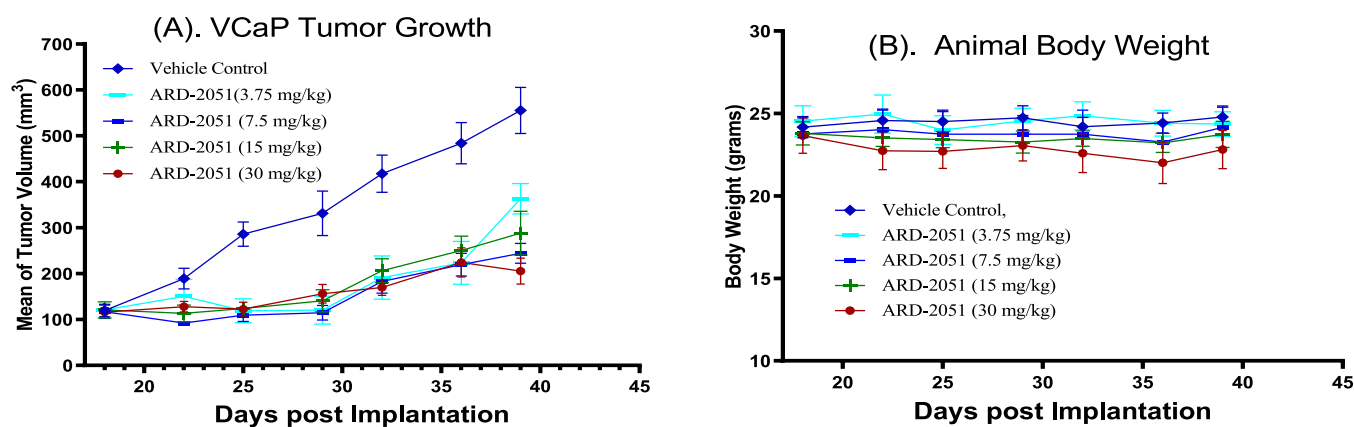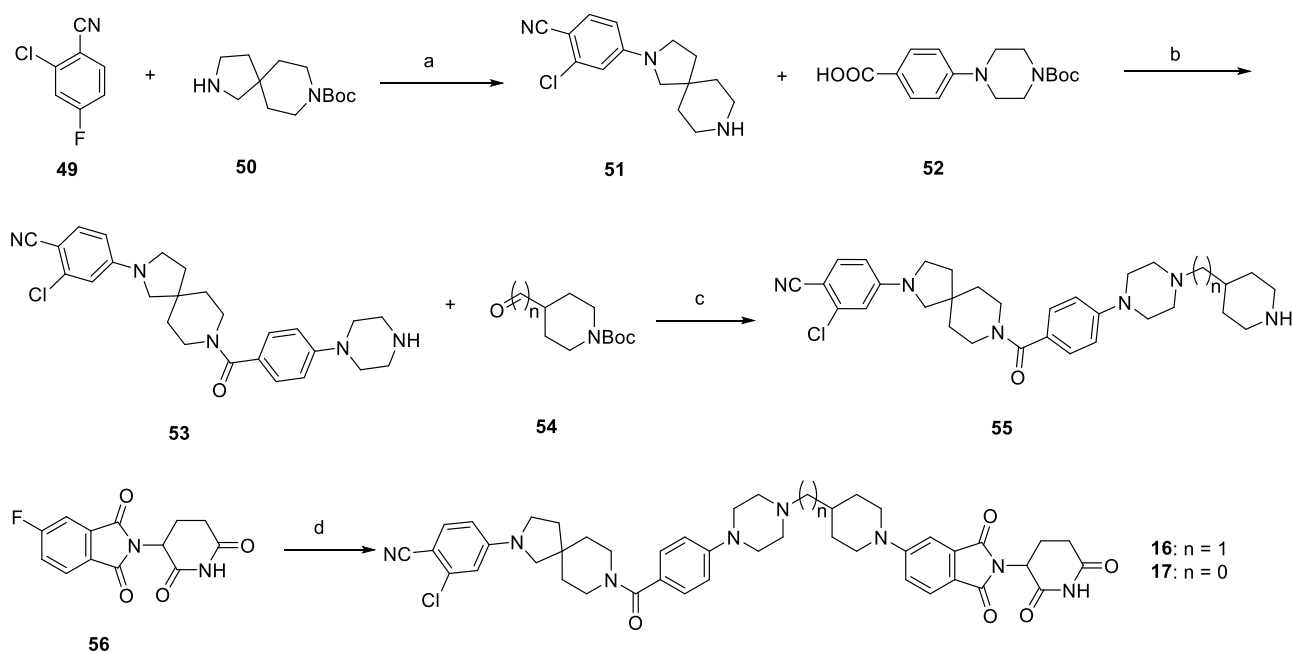
Figure 8. Antitumor activity of ARD-2051 in the VCaP xenograft tumor model in SCID mice. ARD-2051 was dosed via oral gavage daily for a total of 21 days. (A) Tumor growth. (B) Animal body weight.

Scheme 1. Synthesis of Compounds 16 and 17[a]

[a](a) DIPEA, DMSO, 100 °C; TFA, DCM, r.t.; (b) HATU, DIPEA, DMF, r.t.; TFA, DCM, r.t.; (c) NaBH(OAc)₃, AcOH, DCE, r.t.; TFA, DCM, r.t.; (d) DIPEA, DMSO, 100 °C.

still retains good drug exposure in both plasma and tumor tissue at 6 and 24 h time-points. Furthermore, the drug exposure data indicated that ARD-2051 has a good tissue penetration, consistent with its PK data in mice.

Antitumor Activity of ARD-2051 in the VCaP Xenograft Model in Mice. Based upon its promising PD data for ARD-2051, we determined its antitumor activity in the VCaP tumor model, which has an AR gene amplification and is resistant to enzalutamide.

Our efficacy data showed that ARD-2051 effectively inhibited tumor growth at all the 4 doses tested (3.75, 7.5, 15, and 30 mg/kg) (Figure 8). At the end of the 21-day treatment, ARD-2051 inhibited tumor growth by 44, 71, 61, and 80% over the vehicle control treatment, respectively, at 3.75, 7.5, 15, and 30 mg/kg, respectively. Of significance, ARD-2051 caused no signs of toxicity and less than 5% of weight loss at all the doses tested during the entire experiment.

■ CHEMISTRY

Compounds **16** and **17** were prepared, as shown in Scheme 1; compounds **18−29** were prepared, as shown in Scheme 2; and compounds **30−48** and ARi-12 were prepared, as shown in Scheme 3.

In Scheme 1, substitution reaction of compounds **49** with **50** gave intermediate **64** with further subsequent deprotection by TFA. Amidation of compounds **51** with **52** gave the key intermediate **53** after subsequent deprotection by TFA. The intermediate **55** was made by reductive amination of compound **53** with different aldehydes and ketones **54** and subsequent deprotection by TFA. The target compounds were obtained by the substitution reaction of compounds **55** with 2-(2,6-dioxopiperidin-3-yl)-5-fluoroisoindoline-1,3-dione **56**.

In Scheme 2, substitution reaction of compounds **51** with **57** gave intermediate **59** with further subsequent deprotection by TFA. Amidation of compounds **58** with **59** gave the key intermediate **60** after subsequent deprotection by TFA. The

Scheme 2. Synthesis of Compounds 18−29[a]
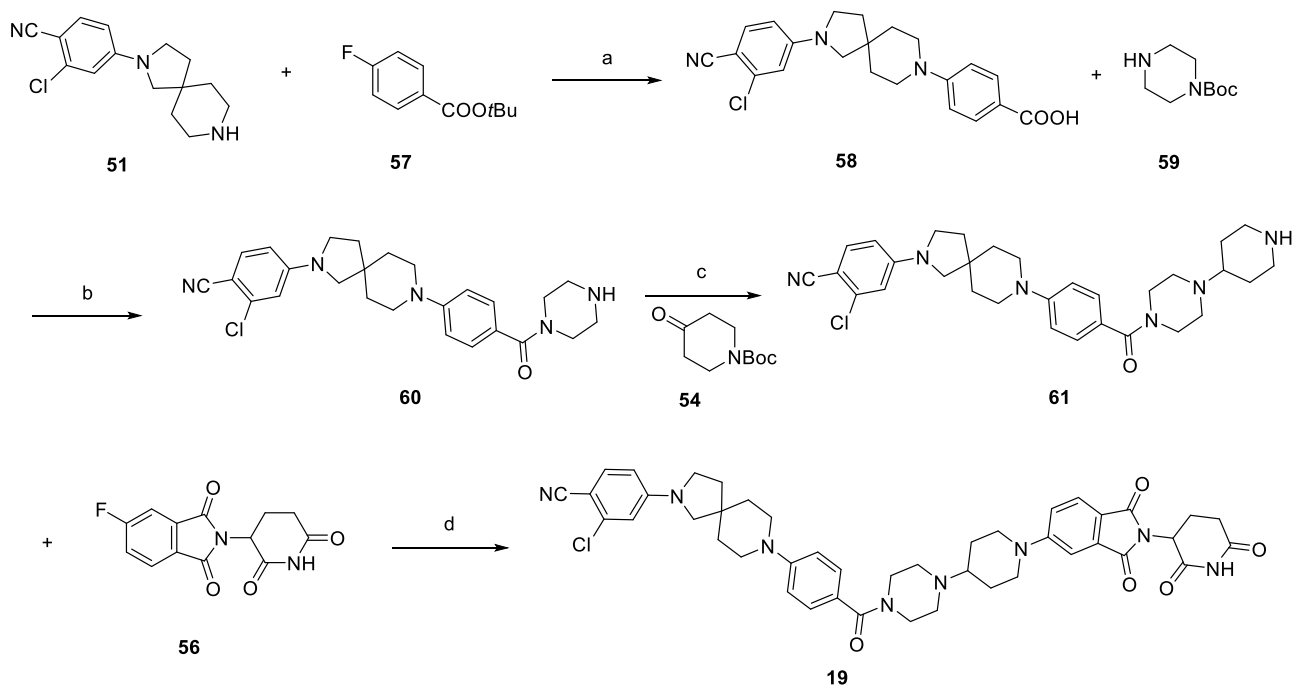
[a](a) DIPEA, DMSO, 100 °C; TFA, DCM, r.t.; (b) HATU, DIPEA, DMF, r.t.; TFA, DCM, r.t.; (c) NaBH(OAc)$_3$, AcOH, DCE, r.t.; TFA, DCM, r.t.; (d) DIPEA, DMSO, 100 °C.

intermediate **61** was made by reductive amination of compound **60** with ketone **54** and subsequent deprotection by TFA. The target compounds were obtained by the substitution reaction of compound **61** with 2-(2,6-dioxopiperidin-3-yl)-5-fluoroisoindoline-1,3-dione **56**.

In Scheme 3, compound **65** was synthesized by the reaction of compounds **62** and **63** with following protection reaction by MsCl. Key intermediate **66** was synthesized by the cyclization reaction of compound **65**. Substitution reaction of compounds **49** with **66** gave intermediate **67** with further subsequent deprotection by TFA. Then, substitution reaction of compounds **67** with **57** gave intermediate **68** with further subsequent deprotection by TFA. Amidation of compounds **68** with **69** gave the key intermediate **69** after subsequent deprotection by TFA. The intermediate **71** was made by reductive amination of compound **69** with ketone **70** and subsequent deprotection by TFA. The target compounds were obtained by the substitution reaction of compounds **71** with 2-(2,6-dioxopiperidin-3-yl)-5-fluoroisoindoline-1,3-dione **56**.
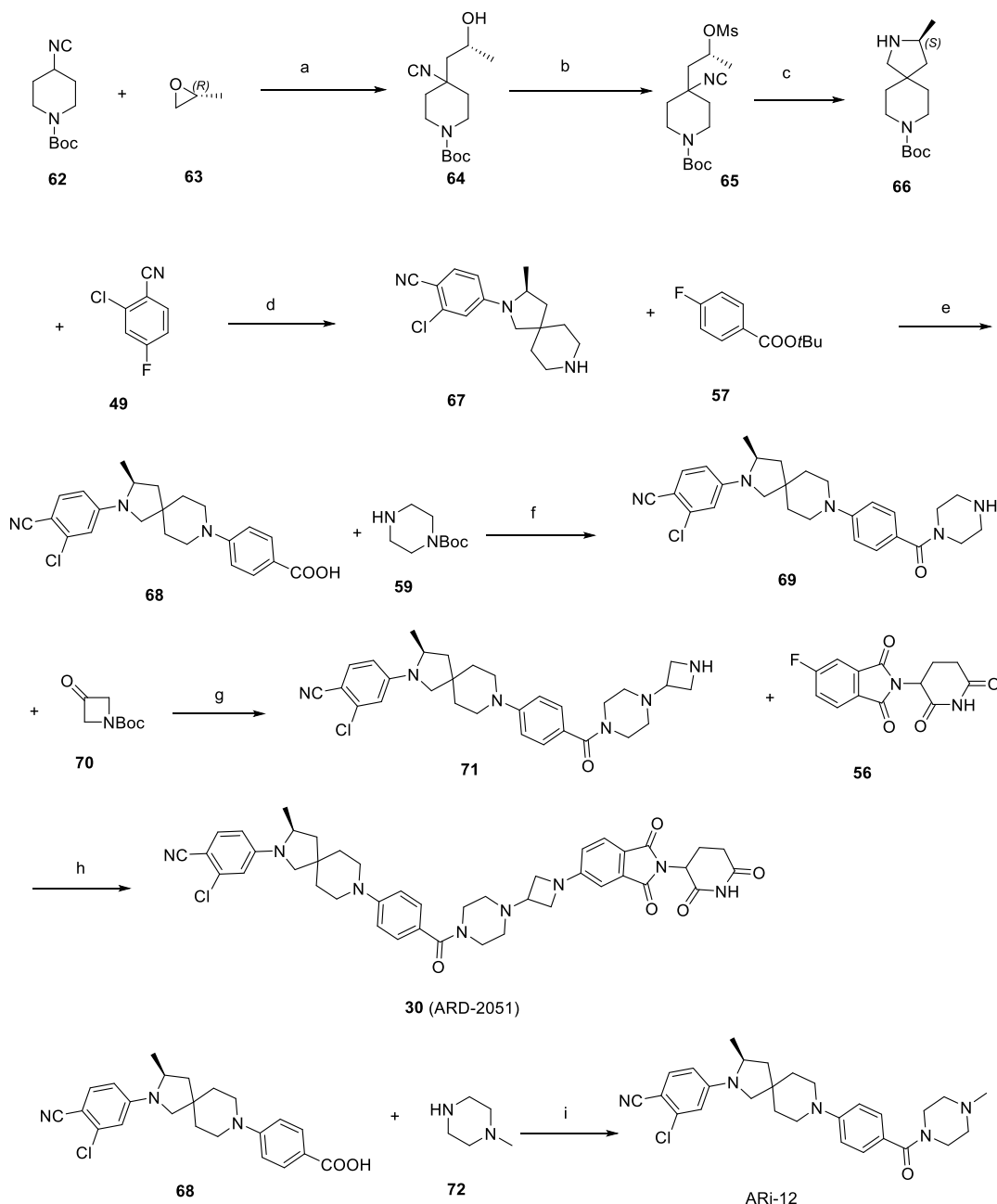
SUMMARY

In this study, we present the discovery and extensive evaluation of a new class of AR PROTAC degraders with ARD-2051 identified as the best compound. We first designed a new class of AR ligands and used them to design a series of PROTAC AR degraders using thalidomide to recruit cereblon/cullin 4A for AR degradation. Extensive optimization of the linker has yielded a series of very potent AR degraders. Further optimization of the AR antagonist portion and the linker portion led to the discovery of ARD-2051 as a highly potent and orally efficacious AR degrader. ARD-2051 achieves DC$_{50}$ values of 0.6 nM in the LNCaP cell line carrying AR T878A mutation and in the VCaP cell line with an AR gene amplification. A mechanistic investigation showed that ARD-2051 is a bona fide AR degrader, consistent with its design. Proteomic analysis revealed that ARD-2051 is a highly selective AR degrader. ARD-2051 potently suppresses expression of AR-regulated genes and effectively inhibits cell growth in LNCaP and VCaP cell lines with low nanomolar potencies. ARD-2051 displays excellent microsomal, hepatocyte, and plasma stability and has no CYP inhibition or hERG liability. ARD-2051 has an excellent PK profile in mouse, rat, and dog with 53, 82, and 46% oral bioavailability, respectively. In comparison, ARD-2051 achieves much improved oral bioavailability in the rat over our previously reported orally active AR degrader ARD-2585. A single oral dose of ARD-2051 at 12.5 mg/kg effectively reduces the levels of AR protein in the VCaP tumor in mice with a strong effect that persisted for at least 24 h and suppresses AR-regulated genes in the VCaP tumor tissue. ARD-2051 effectively inhibits VCaP tumor growth at doses of 3.75−30 mg/kg with oral administration and shows no sign of toxicity in mice at the dose-ranges tested. This study demonstrates that ARD-2051 is a promising development candidate for advanced preclinical studies as a new therapy for the treatment of castration-resistant PCa.

EXPERIMENTAL SECTION

Chemistry. *General Experiment and Information.* Unless otherwise noted, all purchased reagents were used as received without further purification. ^{1}H NMR and ^{13}C NMR spectra were recorded on a Bruker Advance 400 MHz spectrometer. ^{1}H NMR spectra are reported in parts per million (ppm) downfield from tetramethylsilane (TMS). All ^{13}C NMR spectral peaks are reported in ppm and measured with ^{1}H decoupling. In reported spectral data, the format (δ) chemical shift (multiplicity, *J* values in Hz, integration) was used with the following abbreviations: s = singlet, d = doublet, t = triplet, q = quartet, m = multiplet. Mass spectrometric (MS) analysis was carried out with a Waters UPLC mass spectrometer. The final compounds were all purified by C18 reverse phase preparative HPLC column with solvent A (0.1% TFA in H$_2$O) and solvent B (0.1% TFA

Scheme 3. Synthesis of Compounds 30−48 and ARi-12[a]

[a](a) LDA, THF, −78 to 0 °C; (b) MsCl, TEA, DMAP, DCM, 0 °C; (c) LiAlH$_4$, THF, r.t.; (d) DIPEA, DMSO, 100 °C; TFA, DCM, r.t.; (e) DIPEA, DMSO, 100 °C; TFA, DCM, r.t.; (f) HATU, DIPEA, DMF, r.t.; TFA, DCM, r.t.; (g) NaBH(OAc)$_3$, AcOH, DCE, r.t.; TFA, DCM, r.t.; (h) DIPEA, DMSO, 100 °C; (i) HATU, DIPEA, DMF, r.t.

in CH$_3$CN) as eluents. The purity of all the final compounds was shown to be >95% by UPLC−MS or UPLC.

General Procedure for Synthesis of Compounds 16−17. DIPEA (3 equiv) was added to a solution of compounds 49 and 50 (1.1 equiv each) in DMSO. After stirring at 100 °C for 4 h, water was added, the reaction mixture was extracted with EtOAc and washed with water, and the organic phase was dried over Na$_2$SO$_4$. The compound 51 was obtained by removing the solvent under vacuum and purified by flash column with further subsequent deprotection by TFA (80% yield two steps). 2-Chloro-4-(2,8-diazaspiro[4.5]decan-2-yl)benzonitrile (INT-51). ^{1}H NMR (400 MHz, DMSO-d_6): δ 8.80 (s, 1H), 7.58 (d, J = 8.8 Hz, 1H), 6.71 (d, J = 2.2 Hz, 1H), 6.56 (dd, J = 8.9, 2.3 Hz, 1H), 3.40 (t, J = 7.0 Hz, 2H), 3.29 (s, 2H), 3.22−3.02 (m, 4H), 1.93 (t, J = 7.0 Hz, 2H), 1.77−1.66 (m, 4H). UPLC−MS calculated for C$_{15}$H$_{19}$ClN$_3$

[M + H]$^+$, 276.13; found, 276.10. UPLC-retention time: 1.8 min, purity >95%.

DIPEA (5 equiv) and HATU (1.2 equiv) were added to a solution of the compound 51 (1 mmol) and 52 (1.1 equiv) in DMF (2 mL). After 30 min at rt, the mixture was subjected to HPLC purification to afford compound 53 in 82% yield after deprotection in TFA/DCM. 2-Chloro-4-(8-(4-(piperazin-1-yl)benzoyl)-2,8-diazaspiro[4.5]decan-2-yl)benzonitrile (INT-53). ^{1}H NMR (400 MHz, DMSO-d_6): δ 9.13 (s, 1H), 7.58 (d, J = 8.8 Hz, 1H), 7.32 (d, J = 8.7 Hz, 2H), 7.02 (d, J = 8.8 Hz, 2H), 6.71 (d, J = 2.2 Hz, 1H), 6.56 (dd, J = 8.9, 2.2 Hz, 1H), 3.63−3.36 (m, 10H), 3.27 (s, 6H), 1.92 (t, J = 6.9 Hz, 2H), 1.55 (s, 4H). UPLC−MS calculated for C$_{26}$H$_{31}$ClN$_5$O [M + H]$^+$, 464.22; found, 464.24. UPLC-retention time: 3.2 min, purity >95%.

A solution of compound **53** and a series of aldehydes or ketones **54** were added to AcOH (10%) in DCE. After the mixture was stirred at rt for 10 min, NaBH(OAc)$_3$ (1.2 equiv) was added and the mixture was stirred at rt for another 2 h. Then, the compounds **55** were obtained by removing the solvent under vacuum and purified by a flash column with further subsequent deprotection by TFA (82% yield two steps).

DIPEA (5 equiv) was added to a solution of the compounds **55** and 2-(2,6-dioxopiperidin-3-yl)-5-fluoroisoindoline-1,3-dione **56** (1.1 equiv) in DMSO (2 mL). After 4 h at 80 °C, the mixture was subject to HPLC purification to afford compounds **16–17** with 70–85% yields.

2-Chloro-4-(8-(4-(4-((1-(2-(2,6-dioxopiperidin-3-yl)-1,3-dioxoisoindolin-5-yl)piperidin-4-yl)methyl)piperazin-1-yl)benzoyl)-2,8-diazaspiro[4.5]decan-2-yl)benzonitrile (16). ¹H NMR (400 MHz, DMSO-d_6): δ 11.08 (s, 1H), 9.83 (s, 1H), 7.68 (d, J = 8.5 Hz, 1H), 7.60 (d, J = 8.8 Hz, 1H), 7.38–7.25 (m, 4H), 7.05 (d, J = 8.7 Hz, 2H), 6.73 (d, J = 2.1 Hz, 1H), 6.57 (dd, J = 8.9, 2.1 Hz, 1H), 5.10 (d, J = 5.2 Hz, 1H), 4.10 (d, J = 12.9 Hz, 2H), 3.93 (s, 2H), 3.72–3.40 (m, 8H), 3.28 (s, 2H), 3.22–3.09 (m, 6H), 3.02 (t, J = 11.9 Hz, 2H), 2.94–2.85 (m, 1H), 2.65–2.53 (m, 2H), 2.20 (s, 1H), 2.07–2.00 (m, 1H), 1.96–1.83 (m, 4H), 1.56 (s, 4H), 1.30 (dd, J = 21.6, 10.5 Hz, 2H). ¹³C NMR (100 MHz, DMSO-d_6): δ 173.28 (s), 170.57 (s), 169.54 (s), 168.09 (s), 167.43 (s), 158.98 (s), 155.31 (s), 151.32 (s), 150.64 (s), 136.86 (s), 135.14 (s), 134.51 (s), 129.00 (s), 127.28 (s), 125.48 (s), 118.27 (d, J = 5.6 Hz), 115.25 (s), 112.04 (s), 111.14 (s), 108.46 (s), 96.03 (s), 60.99 (s), 57.38 (s), 51.63 (s), 49.25 (s), 47.21 (s), 46.43 (s), 45.00 (s), 35.44 (s), 31.46 (s), 30.70 (s), 29.10 (s), 22.66 (s). UPLC–MS calculated for C$_{45}$H$_{50}$ClN$_8$O$_5$ [M + H]$^+$, 817.36; found, 817.10. UPLC-retention time: 3.9 min, purity >95%.

2-Chloro-4-(8-(4-(4-(1-(2-(2,6-dioxopiperidin-3-yl)-1,3-dioxoisoindolin-5-yl)piperidin-4-yl)piperazin-1-yl)benzoyl)-2,8-diazaspiro[4.5]decan-2-yl)benzonitrile (17). ¹H NMR (400 MHz, DMSO-d_6): δ 11.09 (s, 1H), 10.16 (s, 1H), 7.71 (d, J = 8.5 Hz, 1H), 7.61 (d, J = 8.8 Hz, 1H), 7.43 (s, 1H), 7.33 (d, J = 8.5 Hz, 3H), 7.04 (d, J = 8.5 Hz, 2H), 6.73 (s, 1H), 6.58 (dd, J = 8.9, 1.6 Hz, 1H), 5.09 (dd, J = 12.9, 5.3 Hz, 1H), 4.27 (d, J = 12.9 Hz, 2H), 3.95 (s, 2H), 3.62 (s, 7H), 3.28 (s, 2H), 3.24–2.85 (m, 8H), 2.64–2.53 (m, 2H), 2.20 (d, J = 11.0 Hz, 2H), 2.08–2.00 (m, 1H), 1.93 (t, J = 6.8 Hz, 2H), 1.73 (dd, J = 21.1, 11.0 Hz, 2H), 1.55 (s, 4H), 1.30–1.19 (m, 1H). ¹³C NMR (100 MHz, DMSO-d_6): δ 173.27 (s), 170.54 (s), 169.54 (s), 168.01 (s), 167.41 (s), 159.11 (s), 158.76 (s), 154.76 (s), 151.31 (s), 150.60 (s), 136.86 (s), 135.12 (s), 134.47 (s), 128.97 (s), 127.39 (s), 125.49 (s), 118.86 (d, J = 26.1 Hz), 118.34 (s), 115.28 (s), 114.96 (s), 112.03 (s), 111.13 (s), 108.84 (s), 96.03 (s), 62.61 (s), 57.38 (s), 49.28 (s), 48.42 (s), 46.41 (s), 45.51 (s), 35.42 (s), 31.46 (s), 25.70 (s), 22.65 (s). UPLC–MS calculated for C$_{44}$H$_{48}$ClN$_8$O$_5$ [M + H]$^+$, 803.35; found, 803.10. UPLC-retention time: 3.6 min, purity >95%.

General Procedure for Synthesis of Compounds 18–29. DIPEA (3 equiv) was added to a solution of compounds **51** and **57** (1.1 equiv each) in DMSO. After stirring at 100 °C for 4 h, water was added, the reaction mixture was extracted with EtOAc and washed with water, and the organic phase was dried over Na$_2$SO$_4$. The compound **58** was obtained by removing the solvent under vacuum and purified by a flash column with further subsequent deprotection by TFA (81% yield two steps).

DIPEA (5 equiv) and HATU (1.2 equiv) were added to a solution of the compound **58** (1 mmol) and **59** (1.1 equiv) in DMF (2 mL). After 30 min at rt, the mixture was subjected to HPLC purification to afford compound **60** in 80% yield after deprotection in TFA/DCM.

A solution of compound **60** and ketone **54** was added to AcOH (10%) in DCE. After the mixture was stirred at rt for 10 min, NaBH(OAc)$_3$ (1.2 equiv) was added and the mixture was stirred at rt for another 2 h. Then, the compound **61** was obtained by removing the solvent under vacuum and purified by flash column with further subsequent deprotection by TFA (78% yield two steps).

DIPEA (5 equiv) was added to a solution of the compounds **61** and 2-(2,6-dioxopiperidin-3-yl)-5-fluoroisoindoline-1,3-dione **56** (1.1 equiv) in DMSO (2 mL). After 4 h at 80 °C, the mixture was subject

to HPLC purification to afford compounds **18–29** with 70–91% yields.

2-Chloro-4-(8-(4-(4-((1-(2-(2,6-dioxopiperidin-3-yl)-1,3-dioxoisoindolin-5-yl)piperidin-4-yl)methyl)piperazine-1-carbonyl)-phenyl)-2,8-diazaspiro[4.5]decan-2-yl)benzonitrile (18). ¹H NMR (400 MHz, DMSO-d_6): δ 11.08 (s, 1H), 9.82 (s, 1H), 7.68 (d, J = 8.5 Hz, 1H), 7.60 (d, J = 8.8 Hz, 1H), 7.37 (d, J = 8.6 Hz, 3H), 7.27 (d, J = 8.6 Hz, 1H), 7.03 (d, J = 8.2 Hz, 2H), 6.74 (s, 1H), 6.59 (d, J = 8.8 Hz, 1H), 5.08 (dd, J = 12.8, 5.4 Hz, 2H), 4.09 (d, J = 12.7 Hz, 2H), 3.42 (dd, J = 12.7, 5.7 Hz, 8H), 3.30 (d, J = 6.3 Hz, 4H), 3.18–2.84 (m, 7H), 2.66–2.48 (m, 3H), 2.15 (s, 1H), 2.06–1.99 (m, 1H), 1.96–1.81 (m, 4H), 1.65 (d, J = 16.0 Hz, 4H), 1.30 (d, J = 22.1, 11.4 Hz, 2H). ¹³C NMR (100 MHz, DMSO-d_6): δ 173.27 (s), 170.56 (s), 169.95 (s), 168.08 (s), 167.42 (s), 159.14 (s), 158.78 (s), 155.30 (s), 152.03 (s), 151.34 (s), 136.86 (s), 135.09 (s), 134.49 (s), 129.68 (s), 125.46 (s), 123.94 (s), 118.28 (s), 114.90 (s), 112.03 (s), 111.12 (s), 108.45 (s), 96.01 (s), 61.20 (s), 57.32 (s), 51.82 (s), 49.25 (s), 47.18 (s), 46.41 (s), 45.85 (s), 35.46 (s), 33.94 (s), 31.45 (s), 30.69 (s), 29.04 (s), 22.66 (s). UPLC–MS calculated for C$_{45}$H$_{50}$ClN$_8$O$_5$ [M + H]$^+$, 817.36; found, 817.19. UPLC-retention time: 4.0 min, purity >95%.

2-Chloro-4-(8-(4-(4-(1-(2-(2,6-dioxopiperidin-3-yl)-1,3-dioxoisoindolin-5-yl)piperidin-4-yl)piperazine-1-carbonyl)phenyl)-2,8-diazaspiro[4.5]decan-2-yl)benzonitrile (19). ¹H NMR (400 MHz, DMSO-d_6): δ 11.09 (s, 1H), 7.70 (d, J = 8.5 Hz, 1H), 7.59 (d, J = 8.8 Hz, 1H), 7.43–7.37 (m, 3H), 7.32 (dd, J = 8.6, 1.8 Hz, 1H), 7.02 (d, J = 8.8 Hz, 2H), 6.73 (d, J = 2.1 Hz, 1H), 6.58 (dd, J = 8.9, 2.2 Hz, 1H), 5.12–5.07 (m, 2H), 4.25 (d, J = 12.4 Hz, 2H), 3.63–3.39 (m, 8H), 3.33–3.20 (m, 6H), 3.06–2.84 (m, 4H), 2.68–2.52 (m, 3H), 2.16 (d, J = 9.6 Hz, 2H), 2.05–1.99 (m, 1H), 1.92 (t, J = 6.9 Hz, 2H), 1.75–1.62 (m, 6H). ¹³C NMR (100 MHz, DMSO-d_6): δ 173.26 (s), 170.55 (s), 169.66 (s), 168.07 (s), 167.42 (s), 155.21 (s), 152.13 (s), 151.35 (s), 136.86 (s), 135.11 (s), 134.49 (s), 129.32 (s), 125.46 (s), 124.86 (s), 118.36 (s), 118.13 (s), 114.55 (s), 112.04 (s), 111.13 (s), 108.27 (s), 95.99 (s), 61.07 (s), 57.37 (s), 49.23 (s), 47.09 (s), 46.44 (s), 45.54 (s), 35.47 (s), 34.09 (s), 31.46 (s), 27.58 (s), 22.68 (s). UPLC–MS calculated for C$_{44}$H$_{48}$ClN$_8$O$_5$ [M + H]$^+$, 803.35; found, 803.25. UPLC-retention time: 3.9 min, purity >95%.

2-Chloro-4-(8-(4-(4-(4-(2-(2,6-dioxopiperidin-3-yl)-1,3-dioxoisoindolin-5-yl)piperazin-1-yl)piperidin-1-yl)benzoyl)-2,8-diazaspiro[4.5]decan-2-yl)benzonitrile (20). ¹H NMR (400 MHz, DMSO-d_6): δ 11.08 (s, 1H), 7.63 (dd, J = 24.1, 8.7 Hz, 2H), 7.30 (dd, J = 22.9, 5.1 Hz, 4H), 6.96 (d, J = 8.8 Hz, 2H), 6.74 (d, J = 2.0 Hz, 1H), 6.59 (dd, J = 8.9, 2.1 Hz, 1H), 5.07 (dd, J = 12.9, 5.4 Hz, 1H), 4.08 (d, J = 12.6 Hz, 2H), 3.53–3.37 (m, 8H), 3.30–3.21 (m, 4H), 3.00–2.84 (m, 3H), 2.57 (dd, J = 16.4, 10.9 Hz, 4H), 2.06–1.99 (m, 1H), 1.93–1.81 (m, 4H), 1.72–1.56 (m, 5H), 1.47 (dd, J = 20.0, 9.8 Hz, 2H), 1.25 (d, J = 10.2 Hz, 2H). UPLC–MS calculated for C$_{44}$H$_{48}$ClN$_8$O$_5$ [M + H]$^+$, 803.35; found, 803.08. UPLC-retention time: 4.0 min, purity >95%.

2-Chloro-4-(8-(4-(4-(1-(2-(2,6-dioxopiperidin-3-yl)-1,3-dioxoisoindolin-5-yl)piperidin-4-yl)-1,4-diazepane-1-carbonyl)phenyl)-2,8-diazaspiro[4.5]decan-2-yl)benzonitrile (21). ¹H NMR (400 MHz, DMSO-d_6): δ 11.08 (s, 1H), 7.68 (d, J = 8.5 Hz, 1H), 7.61 (d, J = 8.8 Hz, 1H), 7.37 (dd, J = 5.5, 3.2 Hz, 3H), 7.28 (dd, J = 8.7, 2.1 Hz, 1H), 7.01 (d, J = 8.9 Hz, 2H), 6.75 (d, J = 2.2 Hz, 1H), 6.60 (dd, J = 8.9, 2.3 Hz, 1H), 5.08 (dd, J = 12.9, 5.4 Hz, 1H), 4.22–4.05 (m, 4H), 3.54 (s, 1H), 3.43 (dd, J = 13.9, 6.9 Hz, 6H), 3.33–3.23 (m, 5H), 3.18–2.82 (m, 9H), 2.62–2.55 (m, 1H), 2.14 (s, 1H), 2.03 (dd, J = 8.9, 3.6 Hz, 1H), 1.93 (t, J = 7.0 Hz, 2H), 1.85 (d, J = 11.4 Hz, 2H), 1.64 (d, J = 16.1 Hz, 4H), 1.30 (dd, J = 22.3, 12.2 Hz, 2H). UPLC–MS calculated for C$_{45}$H$_{50}$ClN$_8$O$_5$ [M + H]$^+$, 817.36; found, 817.39. UPLC-retention time: 3.9 min, purity >95%.

2-Chloro-4-(8-(4-(7-(1-(2-(2,6-dioxopiperidin-3-yl)-1,3-dioxoisoindolin-5-yl)piperidin-4-yl)-3,7-diazabicyclo[3.3.1]nonane-3-carbonyl)phenyl)-2,8-diazaspiro[4.5]decan-2-yl)benzonitrile (22). ¹H NMR (400 MHz, DMSO-d_6): δ 11.08 (s, 1H), 7.72 (d, J = 8.4 Hz, 1H), 7.61 (d, J = 8.4 Hz, 1H), 7.44 (s, 1H), 7.31 (dd, J = 25.9, 7.6 Hz, 3H), 6.98 (d, J = 7.8 Hz, 2H), 6.76 (s, 1H), 6.60 (d, J = 8.6 Hz, 1H), 5.08 (dd, J = 12.8, 5.2 Hz, 1H), 4.29 (d, J = 11.6 Hz, 2H), 3.99 (d, J = 12.3 Hz, 4H), 3.11–2.86 (m, 10H), 2.67–2.55 (m, 5H), 2.29

(d, J = 16.1 Hz, 2H), 2.14 (s, 3H), 2.01–1.66 (m, 12H), 1.23 (dd, J = 16.9, 8.2 Hz, 1H). UPLC–MS calculated for $C_{47}H_{52}ClN_8O_5$ [M + H]$^+$, 843.38; found, 843.11. UPLC-retention time: 3.3 min, purity >95%.

2-Chloro-4-(8-(4-(5-(1-(2-(2,6-dioxopiperidin-3-yl)-1,3-dioxoisoindolin-5-yl)piperidin-4-yl)-1,5-diazocane-1-carbonyl)phenyl)-2,8-diazaspiro[4.5]decan-2-yl)benzonitrile (23). ^{1}H NMR (400 MHz, DMSO-d_6): δ 11.08 (s, 1H), 7.72 (d, J = 8.5 Hz, 1H), 7.61 (d, J = 8.8 Hz, 1H), 7.42 (d, J = 1.9 Hz, 1H), 7.36–7.28 (m, 3H), 6.98 (d, J = 8.8 Hz, 2H), 6.76 (d, J = 2.2 Hz, 1H), 6.62–6.59 (m, 1H), 5.08 (dd, J = 12.9, 5.4 Hz, 1H), 4.25 (d, J = 12.5 Hz, 2H), 3.25 (d, J = 6.4 Hz, 6H), 3.07–2.84 (m, 6H), 2.72–2.57 (m, 6H), 2.36–2.31 (m, 1H), 2.15–1.91 (m, 10H), 1.73–1.60 (m, 6H), 1.29–1.15 (m, 2H). UPLC–MS calculated for $C_{46}H_{52}ClN_8O_5$ [M + H]$^+$, 831.38; found, 831.13. UPLC-retention time: 3.5 min, purity >95%.

2-Chloro-4-(8-(4-(6-(1-(2-(2,6-dioxopiperidin-3-yl)-1,3-dioxoisoindolin-5-yl)piperidin-4-yl)-2,6-diazaspiro[3.3]heptane-2-carbonyl)phenyl)-2,8-diazaspiro[4.5]decan-2-yl)benzonitrile (24). ^{1}H NMR (400 MHz, DMSO-d_6): δ 11.11 (s, 1H), 7.74 (d, J = 8.5 Hz, 1H), 7.64 (d, J = 8.8 Hz, 1H), 7.51–7.42 (m, 3H), 7.31 (d, J = 10.0 Hz, 1H), 7.05 (d, J = 8.2 Hz, 2H), 6.79 (d, J = 1.9 Hz, 1H), 6.66 (dd, J = 8.8, 1.8 Hz, 1H), 4.22 (s, 3H), 3.96–3.85 (m, 1H), 3.87–3.68 (m, 3H), 3.68–3.39 (m, 6H), 3.31 (s, 3H), 3.02–2.85 (m, 4H), 2.67–2.52 (m, 3H), 2.20–1.91 (m, 8H), 1.68 (s, 3H), 1.45–1.21 (m, 3H). UPLC–MS calculated for $C_{45}H_{48}ClN_8O_5$ [M + H]$^+$, 815.35; found, 815.13. UPLC-retention time: 3.9 min, purity >95%.

2-Chloro-4-(8-(4-(2-(1-(2-(2,6-dioxopiperidin-3-yl)-1,3-dioxoisoindolin-5-yl)piperidin-4-yl)-2,6-diazaspiro[3.4]octane-6-carbonyl)phenyl)-2,8-diazaspiro[4.5]decan-2-yl)benzonitrile (25). ^{1}H NMR (400 MHz, DMSO-d_6): δ 11.08 (s, 1H), 7.70 (d, J = 8.5 Hz, 1H), 7.60 (d, J = 8.8 Hz, 1H), 7.48–7.39 (m, 3H), 7.30 (d, J = 10.0 Hz, 1H), 7.00 (d, J = 8.2 Hz, 2H), 6.75 (d, J = 1.9 Hz, 1H), 6.60 (dd, J = 8.8, 1.8 Hz, 1H), 4.20 (s, 3H), 3.95–3.86 (m, 1H), 3.83–3.68 (m, 3H), 3.60–3.35 (m, 8H), 3.29 (s, 3H), 3.00–2.83 (m, 4H), 2.65–2.53 (m, 3H), 2.21–1.92 (m, 8H), 1.66 (s, 3H), 1.43–1.20 (m, 3H). UPLC–MS calculated for $C_{46}H_{50}ClN_8O_5$ [M + H]$^+$, 829.36; found, 829.12. UPLC-retention time: 3.6 min, purity >95%.

2-Chloro-4-(8-(4-(4-((1-(2-(2,6-dioxopiperidin-3-yl)-1,3-dioxoisoindolin-5-yl)azetidin-3-yl)methyl)piperazine-1-carbonyl)phenyl)-2,8-diazaspiro[4.5]decan-2-yl)benzonitrile (26). ^{1}H NMR (400 MHz, DMSO-d_6): δ 11.07 (s, 1H), 8.92 (s, 1H), 7.70–7.60 (m, 2H), 7.36 (d, J = 8.5 Hz, 2H), 7.00 (d, J = 8.6 Hz, 2H), 6.77 (d, J = 12.9 Hz, 1H), 6.66 (d, J = 8.2 Hz, 1H), 6.60 (d, J = 7.5 Hz, 1H), 5.06 (dd, J = 12.8, 5.2 Hz, 1H), 4.26–4.22 (m, 2H), 3.65–3.59 (m, 6H), 3.46–3.40 (m, 6H), 3.29 (s, 5H), 2.87 (d, J = 11.9 Hz, 1H), 2.58 (d, J = 23.4 Hz, 3H), 1.92 (t, J = 6.5 Hz, 2H), 1.65 (s, 5H), 1.30 (s, 4H). UPLC–MS calculated for $C_{43}H_{46}ClN_8O_5$ [M + H]$^+$, 789.33; found, 789.25. UPLC-retention time: 4.1 min, purity >95%.

2-Chloro-4-(8-(4-(4-(1-(2-(2,6-dioxopiperidin-3-yl)-1,3-dioxoisoindolin-5-yl)azetidin-3-yl)piperazine-1-carbonyl)phenyl)-2,8-diazaspiro[4.5]decan-2-yl)benzonitrile (27). ^{1}H NMR (400 MHz, DMSO-d_6): δ 11.09 (s, 1H), 7.74 (d, J = 8.2 Hz, 1H), 7.61 (d, J = 8.8 Hz, 1H), 7.39 (d, J = 8.4 Hz, 2H), 7.04 (d, J = 8.4 Hz, 2H), 6.93 (s, 1H), 6.81–6.74 (m, 2H), 6.60 (d, J = 7.5 Hz, 1H), 5.13–5.07 (m, 2H), 4.32 (dd, J = 30.2, 7.5 Hz, 7H), 3.77 (ddd, J = 35.6, 16.6, 8.9 Hz, 4H), 3.48–3.35 (m, 6H), 3.17 (d, J = 5.8 Hz, 2H), 2.95–2.79 (m, 2H), 2.60 (dd, J = 23.9, 7.9 Hz, 2H), 2.06–2.01 (m, 1H), 1.93 (t, J = 6.9 Hz, 2H), 1.67 (s, 5H), 1.26 (dd, J = 11.5, 5.5 Hz, 1H). ^{13}C NMR (100 MHz, DMSO-d_6): δ 173.26 (s), 170.51 (s), 170.00 (s), 167.80 (s), 167.57 (s), 154.90 (s), 151.38 (s), 136.87 (s), 135.15 (s), 134.19 (s), 129.74 (s), 125.40 (s), 123.71 (s), 118.93 (s), 118.35 (s), 115.58 (s), 114.80 (s), 112.07 (s), 105.71 (s), 95.99 (s), 57.34 (s), 54.48 (s), 53.89 (s), 49.24 (d, J = 12.3 Hz), 46.45 (s), 45.73 (s), 35.50 (s), 33.99 (s), 31.43 (s), 22.65 (s). UPLC–MS calculated for $C_{42}H_{44}ClN_8O_5$ [M + H]$^+$, 775.31; found, 775.16. UPLC-retention time: 4.5 min, purity >95%.

2-Chloro-4-(8-(4-(4-(1-(2-(2,6-dioxopiperidin-3-yl)-1,3-dioxoisoindolin-5-yl)azetidin-3-yl)-1,4-diazepane-1-carbonyl)phenyl)-2,8-diazaspiro[4.5]decan-2-yl)benzonitrile (28). ^{1}H NMR (400 MHz, DMSO-d_6): δ 11.11 (s, 1H), 7.74 (d, J = 10.4 Hz, 1H), 7.61 (d, J = 10.1 Hz, 1H), 7.36 (d, J = 9.9 Hz, 2H), 7.01 (d, J = 9.5 Hz,

3H), 6.78 (s, 2H), 6.67–6.55 (m, 1H), 5.08 (s, 2H), 4.37 (s, 14H), 3.02–2.82 (m, 3H), 2.00 (dd, J = 45.9, 20.6 Hz, 9H), 1.64 (s, 5H), 1.25 (s, 1H). UPLC–MS calculated for $C_{43}H_{46}ClN_8O_5$ [M + H]$^+$, 789.33; found, 789.15. UPLC-retention time: 4.2 min, purity >95%.

2-Chloro-4-(8-(4-(6-(1-(2-(2,6-dioxopiperidin-3-yl)-1,3-dioxoisoindolin-5-yl)azetidin-3-yl)-2,6-diazaspiro[3.3]heptane-2-carbonyl)phenyl)-2,8-diazaspiro[4.5]decan-2-yl)benzonitrile (29). ^{1}H NMR (400 MHz, DMSO-d_6): δ 11.08 (s, 1H), 7.72 (d, J = 8.2 Hz, 1H), 7.61 (d, J = 8.8 Hz, 1H), 7.54–7.47 (m, 2H), 7.03–6.93 (m, 3H), 6.83–6.72 (m, 2H), 6.60 (d, J = 8.8 Hz, 1H), 5.06 (dt, J = 23.0, 11.4 Hz, 1H), 4.38–4.08 (m, 10H), 3.29 (s, 6H), 2.87 (d, J = 11.7 Hz, 1H), 2.64 (d, J = 26.4 Hz, 2H), 2.04–1.99 (m, 1H), 1.92 (t, J = 6.8 Hz, 2H), 1.64 (s, 4H), 1.24 (t, J = 12.7 Hz, 1H). UPLC–MS calculated for $C_{43}H_{44}ClN_8O_5$ [M + H]$^+$, 787.31; found, 787.23. UPLC-retention time: 4.0 min, purity >95%.

General Procedure for Synthesis of Compounds 30–48. A round-bottom flask was charged with diisopropylamine (28.0 g, 0.286 mol, 2 equiv) and anhydrous THF (400 mL) under argon and then cooled to −10 °C. *n*-Butyllithium (0.286 mol, 2 equiv) was added dropwise during this temperature, and the mixture warmed to 0 °C for 15 min. Then the mixture cooled to −78 °C. A solution of Boc-4-cyanopiperidine (62) (30 g, 0.143 mol, 1.0 equiv) in anhydrous THF (100 mL) was added dropwise to the formed lithium diisopropylamide solution. The reaction was stirred at 0 °C for 60 min. Then the reaction was cooled back to −78 °C, and (*R*)-propylene oxide (63) (12.4 g, 1.5 equiv) was added. The reaction then slowly warmed to rt and was stirred for 90 min. The reaction was then cooled to −78 °C, and solid ammonium chloride (60 g) was added. The temperature was maintained at −78 °C, and the mixture was stirred for 60 min; then con. HCl (40 mL) and water (300 mL) were added, and the reaction warmed to rt. Ethyl acetate was added, and the layers were separated. The aqueous layer was extracted with ethyl acetate × 2. The combined organic layers were washed with water, dried over sodium sulfate, filtered, and concentrated in vacuo. Flash column chromatography was then used to provide the title intermediate 64 (57% yield).

A round-bottom flask was charged with compound 64 (14 g, 1.0 equiv) and methylene chloride (100 mL) and then cooled to 0 °C. Triethylamine (7.9 g, 1.5 equiv) and 4-(dimethylamino)-pyridine (0.32 g, 0.05 equiv) were added, followed by MsCl (1.2 equiv). The reaction was stirred at 0 °C for 1 h and then quenched with saturated sodium bicarbonate solution and diluted with methylene chloride. The layers were separated, and the aqueous was extracted with methylene chloride. The combined organic layers were washed with brine, dried over sodium sulfate, filtered, and concentrated in vacuo. Flash column chromatography was used to obtain the title compound 65 as an oil (88% yield).

A round-bottom flask was charged with compound 65 (18.8 g, 1.0 equiv) and anhydrous THF (200 mL) under argon and then cooled to 0 °C. Lithium aluminum hydride powder (5.2 g, 2.5 equiv) was added in portions with great care due to production of H$_2$. The mixture was then warmed to rt and stirred for 2–3 h. Then the reaction was quenched with sequential additions of 10 mL of water, 10 mL of 15% NaOH solution, and then stirred 30 min at rt. Sodium sulfate was added, and the mixture was stirred for 30 min, filtered through celite, and washed sequentially with THF, then ethyl acetate. The filtrate was concentrated and column chromatography was then used to purify compound 66 as an oil (53% yield).

DIPEA (3 equiv) was added to a solution of compounds 49 and 66 (1.1 equiv each) in DMSO. After stirring at 100 °C for 4 h, water was added, the reaction mixture was extracted with EtOAc and washed with water, and the organic phase was dried over Na$_2$SO$_4$. The compound 67 was obtained by removing the solvent under vacuum and purified by flash column with further subsequent deprotection by TFA (81% yield two steps). (*S*)-2-Chloro-4-(3-methyl-2,8-diazaspiro-[4.5]decan-2-yl)benzonitrile (INT-**67**). ^{1}H NMR (400 MHz, DMSO-d_6): δ 7.58 (s, 1H), 6.79 (d, J = 2.3 Hz, 1H), 6.65 (dd, J = 8.9, 2.4 Hz, 1H), 4.01 (dt, J = 12.4, 6.2 Hz, 1H), 3.46 (d, J = 11.0 Hz, 1H), 3.32 (d, J = 11.0 Hz, 1H), 3.11–2.98 (m, 4H), 2.22 (dd, J = 12.9, 7.8 Hz, 1H), 1.83 (t, J = 5.3 Hz, 2H), 1.66–1.52 (m, 3H), 1.18 (d, J = 6.1 Hz,

3H). UPLC−MS calculated for $C_{16}H_{21}ClN_3$ [M + H]$^+$, 290.14; found, 290.10. UPLC-retention time: 1.98 min, purity >95%.

DIPEA (3 equiv) was added to a solution of compounds **67** and **57** (1.1 equiv each) in DMSO. After stirring at 100 °C for 4 h, water was added, the reaction mixture was extracted with EtOAc and washed with water, and the organic phase was dried over Na_2SO_4. The compound **68** was obtained by removing the solvent under vacuum and purified by flash column with further subsequent deprotection by TFA (81% yield two steps). (S)-4-(2-(3-Chloro-4-cyanophenyl)-3-methyl-2,8-diazaspiro[4.5]decan-8-yl)benzoic acid (INT-**68**). ^{1}H NMR (400 MHz, DMSO-d_6): δ 7.78 (d, J = 8.9 Hz, 2H), 7.57 (d, J = 8.8 Hz, 1H), 6.97 (d, J = 9.0 Hz, 2H), 6.78 (d, J = 2.2 Hz, 1H), 6.63 (dd, J = 8.9, 2.2 Hz, 1H), 4.00 (dt, J = 12.7, 6.3 Hz, 1H), 3.41 (t, J = 9.6 Hz, 3H), 3.34−3.22 (m, 3H), 2.22 (dd, J = 12.7, 7.7 Hz, 1H), 1.76−1.63 (m, 2H), 1.56 (dd, J = 12.8, 6.5 Hz, 1H), 1.47 (s, 2H), 1.19 (d, J = 6.0 Hz, 3H). UPLC−MS calculated for $C_{23}H_{25}ClN_3O_2$ [M + H]$^+$, 410.17; found, 410.22. UPLC-retention time: 5.5 min, purity >95%.

DIPEA (5 equiv) and HATU (1.2 equiv) were added to a solution of the compound **68** (1 mmol) and **59** (1.1 equiv) in DMF (2 mL). After 30 min at rt, the mixture was subjected to HPLC purification to afford compound **69** in 80% yield after deprotection in TFA/DCM.

A solution of compound **69** and ketone **70** was added to AcOH (10%) in DCE. After the mixture was stirred at rt for 10 min, $NaBH(OAc)_3$ (1.2 equiv) was added and the mixture was stirred at rt for another 2 h. Then, the compound **71** was obtained by removing the solvent under vacuum and purified by flash column with further subsequent deprotection by TFA (78% yield two steps).

DIPEA (5 equiv) was added to a solution of the compounds **71** and 2-(2,6-dioxopiperidin-3-yl)-5-fluoroisoindoline-1,3-dione **56** (1.1 equiv) in DMSO (2 mL). After 4 h at 80 °C, the mixture was subject to HPLC purification to afford compounds **30**−**48** with 70−91% yields.

2-Chloro-4-((3S)-8-(4-(4-(1-(2-(2,6-dioxopiperidin-3-yl)-1,3-dioxoisoindolin-5-yl)azetidin-3-yl)piperazine-1-carbonyl)phenyl)-3-methyl-2,8-diazaspiro[4.5]decan-2-yl)benzonitrile (30). ^{1}H NMR (400 MHz, DMSO-d_6): δ 11.09 (s, 1H), 7.73 (d, J = 8.3 Hz, 1H), 7.60 (d, J = 8.9 Hz, 1H), 7.38 (d, J = 8.7 Hz, 2H), 7.02 (d, J = 8.8 Hz, 2H), 6.92 (d, J = 1.8 Hz, 1H), 6.82−6.75 (m, 2H), 6.66 (dd, J = 9.0, 2.2 Hz, 1H), 5.08 (dd, J = 12.8, 5.4 Hz, 1H), 4.43−4.21 (m, 5H), 4.12−3.52 (m, 5H), 3.35 (ddt, J = 22.6, 18.3, 8.4 Hz, 10H), 2.94−2.84 (m, 1H), 2.66−2.51 (m, 2H), 2.25 (dd, J = 12.7, 7.7 Hz, 1H), 2.08−1.97 (m, 1H), 1.81−1.68 (m, 2H), 1.56 (dt, J = 33.0, 10.3 Hz, 3H), 1.21 (d, J = 6.0 Hz, 3H). ^{13}C NMR (100 MHz, DMSO-d_6): δ 173.26 (s), 170.51 (s), 170.01 (s), 167.80 (s), 167.58 (s), 159.12 (s), 158.76 (s), 154.92 (s), 152.12 (s), 151.21 (s), 136.87 (s), 135.06 (s), 134.18 (s), 129.71 (s), 125.36 (s), 123.79 (s), 118.88 (s), 118.27 (s), 115.52 (s), 114.79 (s), 112.94 (s), 111.94 (s), 105.66 (s), 96.19 (s), 58.23 (s), 54.43 (s), 53.87 (s), 52.88 (s), 49.20 (d, J = 19.1 Hz), 45.97 (s), 45.53 (s), 44.74 (s), 35.04 (s), 34.37 (s), 31.45 (s), 22.65 (s), 19.85 (s). UPLC−MS calculated for $C_{43}H_{46}ClN_8O_5$ [M + H]$^+$, 789.33; found, 789.15. UPLC-retention time: 4.7 min, purity >95%.

2-Chloro-4-((3R)-8-(4-(4-(1-(2-(2,6-dioxopiperidin-3-yl)-1,3-dioxoisoindolin-5-yl)azetidin-3-yl)piperazine-1-carbonyl)phenyl)-3-methyl-2,8-diazaspiro[4.5]decan-2-yl)benzonitrile (31). ^{1}H NMR (400 MHz, DMSO-d_6): δ 11.09 (s, 1H), 7.73 (d, J = 8.2 Hz, 1H), 7.59 (d, J = 8.8 Hz, 1H), 7.39 (d, J = 8.6 Hz, 2H), 7.05 (d, J = 8.7 Hz, 2H), 6.92 (d, J = 1.3 Hz, 1H), 6.80−6.75 (m, 2H), 6.66 (dd, J = 8.9, 2.0 Hz, 1H), 5.08 (dd, J = 12.8, 5.3 Hz, 1H), 4.33 (dd, J = 22.5, 8.0 Hz, 5H), 4.04 (dd, J = 13.1, 6.5 Hz, 1H), 3.69 (dd, J = 45.7, 23.2 Hz, 4H), 3.47−3.26 (m, 9H), 2.98−2.82 (m, 2H), 2.63−2.52 (m, 2H), 2.25 (dd, J = 12.6, 7.7 Hz, 1H), 2.08−2.00 (m, 1H), 1.82−1.70 (m, 2H), 1.64−1.47 (m, 3H), 1.21 (d, J = 6.0 Hz, 3H). ^{13}C NMR (100 MHz, DMSO-d_6): δ 173.25 (s), 170.50 (s), 169.98 (s), 167.80 (s), 167.57 (s), 163.46 (s), 159.53 (s), 159.16 (s), 158.80 (s), 158.43 (s), 154.91 (s), 151.90 (s), 151.20 (s), 136.86 (s), 135.04 (s), 134.17 (s), 129.70 (s), 129.23 (s), 125.34 (s), 124.12 (s), 120.36 (s), 118.90 (s), 118.25 (s), 117.47 (s), 115.52 (s), 114.99 (s), 114.58 (s), 112.94 (s), 111.93 (s), 111.69 (s), 105.66 (s), 96.21 (s), 58.20 (s), 54.42 (s), 53.83 (s), 52.87 (s), 49.29 (s), 49.08 (s), 46.18 (s), 45.74 (s), 44.73

(s), 43.16 (s), 34.97 (s), 34.30 (s), 31.45 (s), 22.65 (s), 19.82 (s). UPLC−MS calculated for $C_{43}H_{46}ClN_8O_5$ [M + H]$^+$, 789.33; found, 789.11. UPLC-retention time: 4.8 min, purity >95%.

2-Chloro-4-((1S)-8-(4-(4-(1-(2-(2,6-dioxopiperidin-3-yl)-1,3-dioxoisoindolin-5-yl)azetidin-3-yl)piperazine-1-carbonyl)phenyl)-1-methyl-2,8-diazaspiro[4.5]decan-2-yl)benzonitrile (32). ^{1}H NMR (400 MHz, DMSO-d_6): δ 11.08 (s, 1H), 7.73 (d, J = 8.2 Hz, 1H), 7.60 (d, J = 8.8 Hz, 1H), 7.36 (d, J = 8.6 Hz, 2H), 7.00 (d, J = 8.7 Hz, 2H), 6.92 (s, 1H), 6.77 (d, J = 6.7 Hz, 2H), 6.61 (d, J = 8.7 Hz, 1H), 5.08 (dd, J = 12.8, 5.3 Hz, 1H), 4.31 (dd, J = 27.3, 19.5 Hz, 6H), 3.32 (ddd, J = 60.3, 27.9, 18.0 Hz, 12H), 2.87 (d, J = 12.3 Hz, 1H), 2.67−2.53 (m, 3H), 2.10−1.89 (m, 3H), 1.76−1.60 (m, 2H), 1.51 (d, J = 20.0 Hz, 2H), 1.04 (d, J = 6.2 Hz, 3H). UPLC−MS calculated for $C_{43}H_{46}ClN_8O_5$ [M + H]$^+$, 789.33; found, 789.15. UPLC-retention time: 4.1 min, purity >95%.

2-Chloro-4-((1R)-8-(4-(4-(1-(2-(2,6-dioxopiperidin-3-yl)-1,3-dioxoisoindolin-5-yl)azetidin-3-yl)piperazine-1-carbonyl)phenyl)-1-methyl-2,8-diazaspiro[4.5]decan-2-yl)benzonitrile (33). ^{1}H NMR (400 MHz, DMSO-d_6): δ 11.08 (s, 1H), 7.73 (d, J = 8.2 Hz, 1H), 7.59 (d, J = 8.8 Hz, 1H), 7.37 (d, J = 8.4 Hz, 2H), 7.00 (d, J = 8.5 Hz, 2H), 6.92 (s, 1H), 6.77 (d, J = 8.4 Hz, 2H), 6.61 (d, J = 8.4 Hz, 1H), 5.08 (dd, J = 12.7, 5.2 Hz, 1H), 4.34 (d, J = 7.4 Hz, 6H), 3.44−3.11 (m, 12H), 2.87 (d, J = 12.0 Hz, 1H), 2.64−2.52 (m, 3H), 1.97 (ddd, J = 32.3, 17.0, 9.1 Hz, 3H), 1.76−1.60 (m, 2H), 1.49 (s, 2H), 1.04 (d, J = 6.0 Hz, 3H). UPLC−MS calculated for $C_{43}H_{46}ClN_8O_5$ [M + H]$^+$, 789.33; found, 789.15. UPLC-retention time: 4.0 min, purity >95%.

4-((3S)-8-(4-(4-(1-(2-(2,6-Dioxopiperidin-3-yl)-1,3-dioxoisoindolin-5-yl)azetidin-3-yl)piperazine-1-carbonyl)phenyl)-3-methyl-2,8-diazaspiro[4.5]decan-2-yl)-2-(trifluoromethyl)benzonitrile (34). ^{1}H NMR (400 MHz, DMSO-d_6): δ 11.09 (s, 1H), 7.75 (dd, J = 20.5, 8.4 Hz, 2H), 7.37 (d, J = 8.3 Hz, 2H), 7.03−6.95 (m, 3H), 6.92 (d, J = 7.9 Hz, 2H), 6.76 (d, J = 8.2 Hz, 1H), 5.10−5.05 (m, 1H), 4.37−4.08 (m, 9H), 3.77 (s, 3H), 3.50 (d, J = 10.8 Hz, 1H), 3.44−3.35 (m, 3H), 3.30−3.16 (m, 5H), 2.88 (dd, J = 21.8, 9.3 Hz, 1H), 2.64−2.52 (m, 2H), 2.28 (dd, J = 12.5, 7.7 Hz, 1H), 2.06−1.98 (m, 1H), 1.74 (d, J = 11.5 Hz, 2H), 1.61 (dd, J = 12.7, 6.4 Hz, 1H), 1.52 (s, 2H), 1.23 (d, J = 5.8 Hz, 3H). UPLC−MS calculated for $C_{44}H_{46}F_3N_8O_5$ [M + H]$^+$, 823.36; found, 823.25. UPLC-retention time: 4.1 min, purity >95%.

2-(Difluoromethyl)-4-((3S)-8-(4-(4-(1-(2-(2,6-dioxopiperidin-3-yl)-1,3-dioxoisoindolin-5-yl)azetidin-3-yl)piperazine-1-carbonyl)phenyl)-3-methyl-2,8-diazaspiro[4.5]decan-2-yl)benzonitrile (35). ^{1}H NMR (400 MHz, DMSO-d_6): δ 11.09 (s, 1H), 7.70 (dd, J = 24.4, 8.1 Hz, 2H), 7.39 (d, J = 7.1 Hz, 2H), 7.05 (d, J = 8.5 Hz, 2H), 6.93 (s, 2H), 6.80 (d, J = 8.5 Hz, 2H), 5.08 (d, J = 8.0 Hz, 1H), 4.30 (s, 5H), 4.07 (s, 1H), 3.75 (d, J = 36.5 Hz, 4H), 3.37 (dd, J = 31.0, 20.3 Hz, 9H), 2.87 (d, J = 12.4 Hz, 1H), 2.69−2.52 (m, 2H), 2.28 (s, 1H), 2.03 (s, 1H), 1.86−1.45 (m, 5H), 1.23 (d, J = 4.2 Hz, 3H). ^{13}C NMR (100 MHz, DMSO-d_6): δ 173.28 (s), 170.52 (s), 170.01 (s), 167.80 (s), 167.58 (s), 159.11 (s), 158.75 (s), 154.90 (s), 152.00 (s), 150.13 (s), 135.66 (s), 134.17 (s), 129.71 (s), 125.38 (s), 123.96 (s), 118.92 (s), 118.42 (s), 117.44 (s), 115.55 (s), 114.93 (s), 114.41 (d, J = 13.0 Hz), 105.69 (s), 92.65 (s), 58.29 (s), 54.46 (s), 53.86 (s), 52.85 (s), 49.21 (d, J = 17.0 Hz), 46.81−46.19 (m), 45.90 (d, J = 45.8 Hz), 44.64 (s), 34.98 (s), 34.33 (s), 31.43 (s), 22.64 (s), 19.81 (s). UPLC−MS calculated for $C_{44}H_{47}F_2N_8O_5$ [M + H]$^+$, 805.37; found, 805.19. UPLC-retention time: 4.2 min, purity >95%.

4-((3S)-8-(4-(4-(1-(2-(2,6-Dioxopiperidin-3-yl)-1,3-dioxoisoindolin-5-yl)azetidin-3-yl)piperazine-1-carbonyl)phenyl)-3-methyl-2,8-diazaspiro[4.5]decan-2-yl)-2-fluorobenzonitrile (36). ^{1}H NMR (400 MHz, DMSO-d_6): δ 11.09 (s, 1H), 7.73 (d, J = 8.2 Hz, 1H), 7.53 (t, J = 8.4 Hz, 1H), 7.40 (d, J = 8.5 Hz, 2H), 7.05 (d, J = 8.5 Hz, 2H), 6.93 (s, 1H), 6.78 (d, J = 8.3 Hz, 1H), 6.56 (dd, J = 14.9, 11.5 Hz, 2H), 5.09 (dd, J = 12.8, 5.3 Hz, 1H), 4.33 (dd, J = 25.2, 7.9 Hz, 5H), 4.02 (dd, J = 13.0, 6.4 Hz, 1H), 3.75 (d, J = 38.0 Hz, 3H), 3.37 (ddd, J = 35.4, 19.8, 9.0 Hz, 10H), 2.96−2.84 (m, 1H), 2.58 (dd, J = 22.5, 15.7 Hz, 3H), 2.26 (dd, J = 12.7, 7.7 Hz, 1H), 2.09−2.01 (m, 1H), 1.85−1.69 (m, 2H), 1.64−1.47 (m, 3H), 1.22 (d, J = 6.0 Hz, 3H). UPLC−MS calculated for $C_{43}H_{46}ClN_8O_5$ [M + H]$^+$, 773.36; found, 773.17. UPLC-retention time: 4.5 min, purity >95%.

5-((3S)-8-(4-(4-(1-(2-(2,6-Dioxopiperidin-3-yl)-1,3-dioxoisoindolin-5-yl)azetidin-3-yl)piperazine-1-carbonyl)phenyl)-3-methyl-2,8-

diazaspiro[4.5]decan-2-yl)-3-(trifluoromethyl)picolinonitrile (**37**). ^{1}H NMR (400 MHz, DMSO-d_6): δ 11.09 (s, 1H), 8.32 (d, J = 2.4 Hz, 1H), 7.74 (d, J = 8.2 Hz, 1H), 7.38 (d, J = 8.6 Hz, 2H), 7.28 (d, J = 2.3 Hz, 1H), 7.02 (d, J = 8.7 Hz, 2H), 6.93 (d, J = 1.6 Hz, 1H), 6.78 (dd, J = 8.3, 1.8 Hz, 1H), 5.08 (d, J = 7.5 Hz, 1H), 4.41−4.22 (m, 7H), 3.62 (d, J = 11.1 Hz, 2H), 3.50−3.20 (m, 10H), 2.88 (dd, J = 22.8, 8.9 Hz, 1H), 2.58 (dd, J = 19.0, 10.5 Hz, 2H), 2.29 (dd, J = 12.7, 7.7 Hz, 1H), 2.08−1.99 (m, 1H), 1.82−1.72 (m, 2H), 1.63 (dd, J = 12.9, 6.6 Hz, 1H), 1.54 (t, J = 5.0 Hz, 2H), 1.25 (d, J = 6.0 Hz, 3H). ^{13}C NMR (100 MHz, DMSO-d_6): δ 173.26 (s), 170.51 (s), 170.02 (s), 167.80 (s), 167.57 (s), 159.04 (s), 158.67 (s), 154.91 (s), 152.21 (s), 144.72 (s), 138.94 (s), 134.18 (s), 129.72 (s), 125.39 (s), 124.22 (s), 123.64 (s), 121.50 (s), 118.91 (s), 117.42 (s), 116.76 (s), 115.54 (s), 115.39−115.28 (m), 114.94 (d, J = 48.2 Hz), 112.68 (s), 105.69 (s), 57.79 (s), 54.47 (s), 53.89 (s), 53.07 (s), 49.22 (d, J = 14.5 Hz), 45.86 (s), 45.38 (s), 44.64 (s), 34.94 (s), 34.17 (s), 31.45 (s), 22.65 (s), 19.50 (s). UPLC−MS calculated for C$_{43}$H$_{45}$F$_3$N$_9$O$_5$ [M + H]$^+$, 824.35; found, 824.23. UPLC-retention time: 4.6 min, purity >95%.

2-Chloro-4-((3S)-8-(4-(4-((1-(2-(2,6-dioxopiperidin-3-yl)-1,3-dioxoisoindolin-5-yl)piperidin-4-yl)methyl)piperazine-1-carbonyl)phenyl)-3-methyl-2,8-diazaspiro[4.5]decan-2-yl)benzonitrile (**38**). ^{1}H NMR (400 MHz, DMSO-d_6): δ 11.08 (s, 1H), 9.80 (s, 1H), 7.68 (d, J = 8.5 Hz, 1H), 7.60 (d, J = 8.8 Hz, 1H), 7.36 (d, J = 8.2 Hz, 3H), 7.28 (d, J = 8.8 Hz, 1H), 6.99 (d, J = 8.4 Hz, 2H), 6.80 (s, 1H), 6.67 (d, J = 8.6 Hz, 1H), 5.13−5.05 (m, 1H), 4.07 (dd, J = 21.0, 9.6 Hz, 5H), 3.61−3.29 (m, 10H), 3.17−2.82 (m, 9H), 2.57 (dd, J = 17.1, 10.9 Hz, 2H), 2.25 (dd, J = 12.5, 7.9 Hz, 1H), 2.15 (s, 1H), 2.06−1.99 (m, 1H), 1.85 (d, J = 11.5 Hz, 2H), 1.74 (s, 2H), 1.62−1.57 (m, 1H), 1.50 (s, 2H), 1.36−1.27 (m, 2H), 1.21 (d, J = 5.8 Hz, 3H). UPLC−MS calculated for C$_{46}$H$_{52}$ClN$_8$O$_5$ [M + H]$^+$, 831.38; found, 831.17. UPLC-retention time: 4.4 min, purity >95%.

2-Chloro-4-((3S)-8-(4-(4-(1-(2-(2,6-dioxopiperidin-3-yl)-1,3-dioxoisoindolin-5-yl)piperidin-4-yl)piperazine-1-carbonyl)phenyl)-3-methyl-2,8-diazaspiro[4.5]decan-2-yl)benzonitrile (**39**). ^{1}H NMR (400 MHz, DMSO-d_6): δ 11.08 (s, 1H), 10.16 (s, 1H), 7.71 (d, J = 8.5 Hz, 1H), 7.60 (d, J = 8.8 Hz, 1H), 7.44−7.31 (m, 4H), 6.98 (d, J = 8.8 Hz, 2H), 6.80 (d, J = 2.1 Hz, 1H), 6.66 (dd, J = 8.9, 2.1 Hz, 1H), 5.11−5.06 (m, 1H), 4.26 (d, J = 12.6 Hz, 4H), 4.04 (d, J = 13.1, 6.5 Hz, 1H), 3.42 (ddd, J = 32.8, 27.3, 11.0 Hz, 10H), 2.94 (ddd, J = 31.5, 21.0, 9.4 Hz, 4H), 2.67−2.53 (m, 3H), 2.24 (dd, J = 12.6, 7.7 Hz, 1H), 2.14 (d, J = 10.0 Hz, 2H), 2.06−1.99 (m, 1H), 1.72 (dd, J = 17.2, 8.3 Hz, 4H), 1.62−1.56 (m, 1H), 1.50 (s, 2H), 1.30−1.24 (m, 1H), 1.21 (d, J = 6.0 Hz, 3H). UPLC−MS calculated for C$_{45}$H$_{50}$ClN$_8$O$_5$ [M + H]$^+$, 817.36; found, 817.1.0. UPLC-retention time: 4.3 min, purity >95%.

2-Chloro-4-((3S)-8-(4-(4-((1-(2-(2,6-dioxopiperidin-3-yl)-1,3-dioxoisoindolin-5-yl)piperidin-4-yl)methyl)piperazine-1-carbonyl)-phenyl)-3-methyl-2,8-diazaspiro[4.5]decan-2-yl)benzonitrile (**40**). ^{1}H NMR (400 MHz, DMSO-d_6): δ 11.10 (s, 1H), 9.51 (s, 1H), 7.78 (d, J = 8.4 Hz, 1H), 7.60 (d, J = 8.8 Hz, 1H), 7.51 (s, 1H), 7.34 (dd, J = 25.8, 8.2 Hz, 3H), 7.06 (d, J = 8.2 Hz, 2H), 6.80 (s, 1H), 6.67 (d, J = 8.8 Hz, 1H), 5.13−5.09 (m, 1H), 4.31−3.95 (m, 5H), 3.62 (s, 2H), 3.47−3.09 (m, 13H), 3.01−2.84 (m, 3H), 2.58 (dd, J = 18.9, 13.0 Hz, 3H), 2.26 (dd, J = 12.6, 7.8 Hz, 1H), 2.16 (s, 1H), 2.07−2.00 (m, 1H), 1.78 (s, 4H), 1.64−1.51 (m, 3H), 1.21 (d, J = 5.8 Hz, 3H). ^{13}C NMR (100 MHz, DMSO-d_6): δ 173.26 (s), 170.49 (s), 169.68 (s), 167.89 (s), 167.37 (s), 159.03 (s), 158.66 (s), 154.58 (s), 151.21 (s), 136.86 (s), 135.07 (s), 134.28 (s), 129.08 (s), 125.48 (s), 120.43 (s), 119.27 (s), 118.27 (s), 115.45 (s), 112.96 (s), 111.96 (s), 109.48 (s), 96.19 (s), 61.08 (s), 58.17 (s), 52.88 (s), 51.38 (s), 49.36 (s), 44.64 (d, J = 21.3 Hz), 44.25−43.98 (m), 34.95 (s), 34.29 (s), 31.46 (s), 30.90 (s), 30.05 (s), 22.61 (s), 19.86 (s). UPLC−MS calculated for C$_{46}$H$_{52}$ClN$_8$O$_5$ [M + H]$^+$, 831.38; found, 831.10. UPLC-retention time: 4.2 min, purity >95%.

2-Chloro-4-((3S)-8-(4-(4-(1-(2-(2,6-dioxopiperidin-3-yl)-1,3-dioxoisoindolin-5-yl)piperidin-4-yl)piperazine-1-carbonyl)phenyl)-3-methyl-2,8-diazaspiro[4.5]decan-2-yl)benzonitrile (**41**). ^{1}H NMR (400 MHz, DMSO-d_6): δ 11.10 (s, 1H), 10.07 (s, 1H), 7.77 (d, J = 8.4 Hz, 1H), 7.64−7.49 (m, 2H), 7.42−7.25 (m, 3H), 7.02 (d, J = 8.4 Hz, 2H), 6.80 (s, 1H), 6.66 (d, J = 7.2 Hz, 1H), 5.11 (dd, J = 12.8, 5.3

Hz, 1H), 4.26 (s, 3H), 4.04 (dd, J = 12.4, 6.0 Hz, 1H), 3.61 (d, J = 8.4 Hz, 2H), 3.35 (ddd, J = 42.1, 31.4, 7.5 Hz, 10H), 3.06−2.80 (m, 3H), 2.64−2.52 (m, 2H), 2.25 (dd, J = 12.5, 7.7 Hz, 1H), 2.17−1.94 (m, 3H), 1.83−1.46 (m, 8H), 1.37−1.25 (m, 1H), 1.21 (d, J = 5.9 Hz, 3H). ^{13}C NMR (100 MHz, DMSO-d_6): δ 173.25 (s), 170.48 (s), 169.85 (s), 167.85 (s), 167.37 (s), 159.06 (s), 158.70 (s), 154.57 (s), 151.72 (s), 151.21 (s), 136.86 (s), 135.06 (s), 134.24 (s), 129.25 (s), 125.43 (s), 120.54 (s), 119.30 (s), 118.27 (s), 115.00 (s), 114.70 (s), 112.95 (s), 111.94 (s), 109.47 (s), 99.99 (s), 96.18 (s), 62.84 (s), 58.21 (s), 52.88 (s), 49.35 (s), 48.11 (s), 46.20 (s), 44.86 (d, J = 20.5 Hz), 35.02 (s), 34.35 (s), 31.45 (s), 26.64 (s), 22.62 (s), 19.86 (s). UPLC−MS calculated for C$_{45}$H$_{50}$ClN$_8$O$_5$ [M + H]$^+$, 817.36; found, 817.20. UPLC-retention time: 4.1 min, purity >95%.

2-Chloro-4-((3S)-8-(4-(1′-(2-(2,6-dioxopiperidin-3-yl)-1,3-dioxoisoindolin-5-yl)-[3,3′-biazetidine]-1-carbonyl)phenyl)-3-methyl-2,8-diazaspiro[4.5]decan-2-yl)benzonitrile (**42**). ^{1}H NMR (400 MHz, DMSO-d_6): δ 11.07 (s, 1H), 7.68−7.49 (m, 5H), 6.97 (s, 2H), 6.83−6.78 (m, 2H), 6.68−6.64 (m, 1H), 5.05 (dd, J = 12.9, 5.4 Hz, 1H), 4.15 (d, J = 8.2 Hz, 2H), 4.05 (d, J = 6.2 Hz, 1H), 3.44−3.24 (m, 8H), 3.11 (dd, J = 12.9, 7.7 Hz, 1H), 3.00 (d, J = 3.7 Hz, 1H), 2.96−2.82 (m, 2H), 2.57 (dd, J = 14.9, 11.0 Hz, 3H), 2.24 (dd, J = 12.6, 7.8 Hz, 1H), 2.07−1.96 (m, 2H), 1.73 (s, 2H), 1.60−1.55 (m, 1H), 1.50 (d, J = 9.3 Hz, 2H), 1.20 (d, J = 6.0 Hz, 3H). UPLC−MS calculated for C$_{42}$H$_{43}$ClN$_7$O$_5$ [M + H]$^+$, 760.30; found, 760.47. UPLC-retention time: 5.8 min, purity >95%.

2-Chloro-4-((3S)-8-(4-(4-((1-(2-(2,6-dioxopiperidin-3-yl)-1,3-dioxoisoindolin-5-yl)azetidin-3-yl)methyl)piperazine-1-carbonyl)phenyl)-3-methyl-2,8-diazaspiro[4.5]decan-2-yl)benzonitrile (**43**). ^{1}H NMR (400 MHz, DMSO-d_6): δ 11.08 (s, 1H), 7.68 (d, J = 8.3 Hz, 1H), 7.59 (d, J = 8.9 Hz, 1H), 7.39 (d, J = 8.8 Hz, 2H), 7.04 (d, J = 8.8 Hz, 2H), 6.79 (d, J = 1.9 Hz, 2H), 6.68−6.65 (m, 2H), 5.11−5.03 (m, 1H), 4.24 (t, J = 8.2 Hz, 2H), 4.03 (dd, J = 13.2, 6.6 Hz, 1H), 3.85 (dd, J = 8.2, 5.9 Hz, 2H), 3.54 (d, J = 6.8 Hz, 2H), 3.48−3.17 (m, 14H), 2.89 (ddd, J = 17.4, 14.1, 5.4 Hz, 1H), 2.64−2.47 (m, 3H), 2.27−2.21 (m, 1H), 2.05−1.99 (m, 1H), 1.76 (dd, J = 10.5, 6.6 Hz, 2H), 1.62−1.50 (m, 3H), 1.21 (d, J = 6.0 Hz, 3H). ^{13}C NMR (101 MHz, DMSO-d_6): δ 173.26 (s), 170.54 (s), 169.92 (s), 167.90 (s), 167.61 (s), 159.18 (s), 158.82 (s), 155.41 (s), 151.92 (s), 151.19 (s), 136.86 (s), 135.04 (s), 134.25 (s), 129.70 (s), 125.32 (s), 124.03 (s), 118.25 (s), 117.85 (s), 114.87 (d, J = 16.0 Hz), 112.93 (s), 111.92 (s), 104.98 (s), 96.21 (s), 58.89 (s), 58.22 (s), 55.69 (s), 52.87 (s), 51.31 (s), 49.24 (s), 46.46−46.18 (m), 45.94 (d, J = 44.6 Hz), 44.73 (s), 34.97 (s), 34.30 (s), 31.45 (s), 25.20 (s), 22.67 (s), 19.82 (s). UPLC−MS calculated for C$_{44}$H$_{48}$ClN$_8$O$_5$ [M + H]$^+$, 803.35; found, 803.07. UPLC-retention time: 4.6 min, purity >95%.

2-Chloro-4-((3S)-8-(4-((1S,4S)-5-(1-(2-(2,6-dioxopiperidin-3-yl)-1,3-dioxoisoindolin-5-yl)azetidin-3-yl)-2,5-diazabicyclo[2.2.1]-heptane-2-carbonyl)phenyl)-3-methyl-2,8-diazaspiro[4.5]decan-2-yl)benzonitrile (**44**). ^{1}H NMR (400 MHz, DMSO-d_6): δ 11.08 (s, 1H), 7.72 (d, J = 8.2 Hz, 1H), 7.60 (d, J = 8.9 Hz, 1H), 7.45 (d, J = 6.5 Hz, 2H), 6.97 (d, J = 8.7 Hz, 2H), 6.90 (s, 1H), 6.80 (d, J = 2.1 Hz, 1H), 6.75 (d, J = 8.0 Hz, 1H), 6.66 (dd, J = 8.9, 2.1 Hz, 1H), 5.08 (dd, J = 12.9, 5.3 Hz, 1H), 4.48−4.31 (m, 4H), 4.24−4.13 (m, 2H), 4.06−4.02 (m, 1H), 3.46−3.23 (m, 8H), 2.93−2.84 (m, 1H), 2.64−2.52 (m, 2H), 2.24 (dd, J = 12.7, 7.8 Hz, 3H), 2.06−1.99 (m, 1H), 1.77−1.67 (m, 2H), 1.58 (dd, J = 12.8, 6.5 Hz, 1H), 1.49 (s, 2H), 1.21 (d, J = 6.0 Hz, 3H). ^{13}C NMR (100 MHz, DMSO-d_6): δ 173.26 (s), 170.51 (s), 167.80 (s), 167.57 (s), 158.90 (s), 158.57 (s), 154.84 (s), 152.76 (s), 151.21 (s), 136.86 (s), 135.07 (s), 134.17 (s), 129.78 (s), 125.36 (s), 118.78 (s), 118.27 (s), 115.47 (s), 114.18 (s), 112.94 (s), 111.95 (s), 105.60 (s), 96.16 (s), 58.26 (s), 52.88 (s), 49.27 (s), 45.57 (s), 45.12 (s), 44.79 (s), 35.05 (s), 34.36 (s), 31.45 (s), 22.65 (s), 19.87 (s). UPLC−MS calculated for C$_{44}$H$_{46}$ClN$_8$O$_5$ [M + H]$^+$, 801.33; found, 801.54. UPLC-retention time: 4.5 min, purity >95%.

2-Chloro-4-((3S)-8-(4-((1R,4R)-5-(1-(2-(2,6-dioxopiperidin-3-yl)-1,3-dioxoisoindolin-5-yl)azetidin-3-yl)-2,5-diazabicyclo[2.2.1]-heptane-2-carbonyl)phenyl)-3-methyl-2,8-diazaspiro[4.5]decan-2-yl)benzonitrile (**45**). ^{1}H NMR (400 MHz, DMSO-d_6): δ 11.08 (s, 1H), 7.72 (d, J = 8.3 Hz, 1H), 7.60 (d, J = 8.9 Hz, 1H), 7.45 (d, J = 6.0 Hz, 2H), 6.97 (d, J = 8.8 Hz, 2H), 6.90 (s, 1H), 6.80 (d, J = 2.2 Hz, 1H), 6.75 (d, J = 8.1 Hz, 1H), 6.66 (dd, J = 9.0, 2.3 Hz, 1H), 5.08

(dd, J = 12.9, 5.4 Hz, 1H), 4.79−4.59 (m, 1H), 4.50−4.30 (m, 4H), 4.24 (s, 1H), 4.15 (d, J = 7.1 Hz, 1H), 4.04 (dd, J = 13.3, 6.6 Hz, 1H), 3.45−3.22 (m, 8H), 2.89 (ddd, J = 17.4, 14.2, 5.4 Hz, 1H), 2.64−2.51 (m, 2H), 2.24 (dd, J = 12.7, 7.7 Hz, 3H), 2.03 (dd, J = 8.9, 3.6 Hz, 1H), 1.77−1.66 (m, 2H), 1.58 (dd, J = 12.8, 6.5 Hz, 1H), 1.49 (s, 2H), 1.21 (d, J = 6.1 Hz, 3H). UPLC−MS calculated for $C_{44}H_{46}ClN_8O_5$ $[M + H]^+$, 801.33; found, 801.44. UPLC-retention time: 4.5 min, purity >95%.

2-Chloro-4-((3S)-8-(4-(4-(1-(2-(2,6-dioxopiperidin-3-yl)-1,3-dioxoisoindolin-5-yl)azetidin-3-yl)piperidine-1-carbonyl)phenyl)-3-methyl-2,8-diazaspiro[4.5]decan-2-yl)benzonitrile (46). ^{1}H NMR (400 MHz, DMSO-d_6): δ 11.07 (s, 1H), 7.60 (dd, J = 16.8, 8.6 Hz, 2H), 7.35 (d, J = 8.5 Hz, 2H), 7.17 (d, J = 8.6 Hz, 2H), 6.76 (dd, J = 13.5, 1.8 Hz, 2H), 6.63 (ddd, J = 10.2, 8.7, 1.9 Hz, 2H), 5.05 (dd, J = 12.8, 5.4 Hz, 1H), 4.04 (dt, J = 13.3, 7.4 Hz, 3H), 3.79−3.70 (m, 2H), 3.47−3.29 (m, 6H), 2.96−2.76 (m, 3H), 2.64−2.52 (m, 3H), 2.25 (dd, J = 12.7, 7.7 Hz, 1H), 2.04−1.96 (m, 1H), 1.66 (ddd, J = 29.5, 18.8, 14.6 Hz, 9H), 1.20 (d, J = 6.0 Hz, 3H), 1.07 (d, J = 9.6 Hz, 2H). ^{13}C NMR (100 MHz, DMSO-d_6): δ 173.26 (s), 170.55 (s), 169.38 (s), 167.96 (s), 167.64 (s), 159.12 (s), 158.75 (s), 155.53 (s), 151.15 (s), 149.76 (s), 136.87 (s), 135.02 (s), 134.28 (s), 129.00 (s), 125.25 (s), 118.24 (s), 117.19 (d, J = 14.1 Hz), 116.54 (s), 114.45 (s), 112.94 (s), 111.93 (s), 104.71 (s), 96.26 (s), 58.06 (s), 55.04 (s), 52.86 (s), 49.19 (s), 47.85 (s), 47.43 (s), 44.70 (s), 34.64 (s), 33.99 (s), 31.45 (s), 22.69 (s), 19.78 (s). UPLC−MS calculated for $C_{44}H_{47}ClN_7O_5$ $[M + H]^+$, 788.33; found, 788.38. UPLC-retention time: 6.3 min, purity >95%.

3-(4-(4-((S)-2-(3-Chloro-4-cyanophenyl)-3-methyl-2,8-diazaspiro[4.5]decan-8-yl)benzoyl)piperazin-1-yl)-1-(2-(2,6-dioxopiperidin-3-yl)-1,3-dioxoisoindolin-5-yl)azetidine-3-carbonitrile (47). ^{1}H NMR (400 MHz, DMSO-d_6): δ 11.08 (s, 1H), 7.74 (t, J = 7.0 Hz, 1H), 7.60 (d, J = 8.8 Hz, 1H), 7.33 (dd, J = 11.2, 8.8 Hz, 2H), 6.98 (dd, J = 14.9, 10.7 Hz, 3H), 6.86−6.75 (m, 2H), 6.66 (dd, J = 8.9, 2.1 Hz, 1H), 5.08 (dd, J = 12.9, 5.3 Hz, 1H), 4.47 (d, J = 8.9 Hz, 2H), 4.18 (s, 2H), 3.59 (s, 5H), 3.47−3.17 (m, 9H), 2.90 (dd, J = 22.8, 8.5 Hz, 1H), 2.62−2.52 (m, 2H), 2.27−2.21 (m, 1H), 2.07−1.99 (m, 1H), 1.73 (d, J = 7.8 Hz, 2H), 1.56 (dd, J = 20.1, 13.6 Hz, 3H), 1.21 (d, J = 6.0 Hz, 3H). UPLC−MS calculated for $C_{44}H_{45}ClN_9O_5$ $[M + H]^+$, 814.33; found, 814.39. UPLC-retention time: 5.9 min, purity >95%.

2-Chloro-4-((3S)-8-(4-(3-(4-(2-(2,6-dioxopiperidin-3-yl)-1,3-dioxoisoindolin-5-yl)piperazin-1-yl)azetidine-1-carbonyl)phenyl)-3-methyl-2,8-diazaspiro[4.5]decan-2-yl)benzonitrile (48). ^{1}H NMR (400 MHz, DMSO-d_6): δ 11.10 (s, 1H), 7.76 (t, J = 7.6 Hz, 1H), 7.63−7.49 (m, 4H), 7.38 (d, J = 8.4 Hz, 1H), 7.01 (d, J = 8.8 Hz, 2H), 6.78 (d, J = 1.8 Hz, 1H), 6.65 (dd, J = 8.9, 1.9 Hz, 1H), 5.10 (dd, J = 12.8, 5.3 Hz, 1H), 4.60 (s, 1H), 4.25 (dd, J = 37.2, 13.0 Hz, 3H), 4.02 (dd, J = 13.0, 6.4 Hz, 1H), 3.73 (d, J = 26.0 Hz, 3H), 3.36 (dt, J = 42.4, 12.3 Hz, 10H), 2.93−2.83 (m, 1H), 2.67−2.50 (m, 3H), 2.24 (dd, J = 12.6, 7.7 Hz, 1H), 2.07−1.99 (m, 1H), 1.80−1.68 (m, 2H), 1.61−1.43 (m, 3H), 1.20 (d, J = 5.9 Hz, 3H). ^{13}C NMR (100 MHz, DMSO-d_6): δ 173.27 (s), 170.48 (s), 169.86 (s), 167.86 (s), 167.37 (s), 159.21 (s), 158.85 (s), 158.48 (s), 154.55 (s), 152.74 (s), 151.19 (s), 136.86 (s), 135.02 (s), 134.23 (s), 129.91 (s), 125.41 (s), 121.58 (s), 120.52 (s), 119.38 (s), 118.26 (s), 117.49 (s), 114.53 (d, J = 12.6 Hz), 112.91 (s), 111.91 (s), 109.58 (s), 96.19 (s), 58.22 (s), 54.10 (s), 52.87 (s), 49.35 (s), 48.66 (s), 45.73 (s), 45.28 (s), 44.78 (d, J = 11.3 Hz), 34.61 (d, J = 67.0 Hz), 31.43 (s), 22.61 (s), 19.79 (s). UPLC−MS calculated for $C_{43}H_{46}ClN_8O_5$ $[M + H]^+$, 789.33; found, 789.47. UPLC-retention time: 4.8 min, purity >95%.

(S)-2-Chloro-4-(3-methyl-8-(4-(4-methylpiperazine-1-carbonyl)-phenyl)-2,8-diazaspiro[4.5]decan-2-yl)benzonitrile (ARi-12). ^{1}H NMR (400 MHz, DMSO-d_6): δ 9.94 (s, 1H), 7.60 (d, J = 8.8 Hz, 1H), 7.35 (d, J = 8.4 Hz, 2H), 7.00 (d, J = 8.5 Hz, 2H), 6.80 (s, 1H), 6.67 (d, J = 8.8 Hz, 1H), 4.07−4.02 (m, 2H), 3.57−3.16 (m, 11H), 3.07 (s, 2H), 2.83 (s, 3H), 2.25 (dd, J = 12.5, 7.7 Hz, 1H), 1.74 (d, J = 3.5 Hz, 2H), 1.61−1.53 (m, 1H), 1.50 (s, 2H), 1.21 (d, J = 5.9 Hz, 3H). UPLC−MS calculated for $C_{28}H_{35}ClN_5O$ $[M + H]^+$, 492.26; found, 492.21. UPLC-retention time: 4.2 min, purity >95%.

Computational Modeling. All modeling was conducted using the software package MOE.[41] The AR ligand binding domain in complex with S-1 (PDB ID: 2AXA) retrieved from the RCSB was utilized for conducting docking studies with our designed ligands. The crystal structure obtained from the RCSB was first imported into MOE and prepared for modeling in a standard fashion. Crystallization additives and crystallographic water molecules were removed. Chain breaks if present due to unresolved residues were either capped or built-in using MOE utilities. N- and C-termini were capped with ACE and NME. Missing sidechains were built in using MOE utilities. Bond orders for crystallographic ligands were corrected if necessary. Hydrogen atoms were added, and the systems parameterized using AMBER10[42] as implemented in the MOE package. For each complex, all heavy atoms were fixed, and the positions of the hydrogen atoms were allowed to relax using energy minimization.

Ligands **14a** and **15a** were docked into the 2AXA structure, which is AR in its agonist conformation. Docking was conducted using MOE's template docking method with substructure matching. The crystallographic ligand was used to define the binding site. The maximum common substructure between the crystallographic ligand and the ligand to be docked was used for the substructure matching. This method takes conformations for the ligand to be docked and superimposes them into the protein binding site by aligning it to the substructure of the crystallographic ligand. Once aligned, the crystallographic ligand is removed, and additional conformational sampling of the ligand being docked is conducted. That sampling is followed by energy minimization of the docked ligand, keeping the protein rigid to create a refined pose, which is then scored for ranking. Default settings for MOE were used, except that sampling was increased by increasing the number of placements for refinement, and the level of refinement was increased by changing the energy minimization termination criterion to a minimum value for the gradient and a maximum value for the number of iterations. Ligands to be docked were built into MOE, and hydrogen atoms were added, charged with AMBER 10, and energy-minimized before docking. To provide better substructure matching, the S-1 crystallographic ligand of 2AXA was modified replacing the trifluoromethyl with chlorine and the nitro group with nitrile.

AR Binding Assay. The PolarScreen AR competitor assay kit (ThermoFisher, A15880) was used for AR FP binding assay. Briefly, FP binding assay was performed in 384-well low volume black round bottom microplates (Corning, 4514) using the CLARIOstar microplate reader (BMG Labtech). To each well, 3.6 nM of Fluormone AL Green and 400 nM of AR-LBD protein were added to a final volume of 20 μL in the assay buffer (AR Green assay buffer with 2 mM DTT), with plates covered to protect reagents from light. The plate was incubated at room temperature for 4 h to reach equilibrium. The polarization values in millipolarization (mP) units were measured at an excitation wavelength of 485 nm and an emission wavelength of 530 nm. All experimental data were analyzed using Prism 8.0 software (GraphPad Software). IC_{50} values were determined by nonlinear regression fitting of the competition curves (mP values vs log-[compound]).

Cell Lines and Cell Culture. LNCaP and VCaP human PCa cell lines were purchased from American Type Culture Collection (ATCC). LNCaP cells were grown in RPMI 1640 (Invitrogen), and VCaP cells were grown in DMEM with Glutamax (Invitrogen). Cells were supplemented with 10% fetal bovine serum (Invitrogen) at 37 °C in a humidified 5% CO_2 incubator. Cell viability was evaluated by a WST-8 assay (Dojindo), following the manufacturer's instructions. Western blot analysis was performed as previously described.[33,34]

Quantitative Real-Time Polymerase Chain Reaction. Real-time PCR was performed using QuantStudio 7 Flex real-time PCR system as described previously.[33,34] Briefly, RNA was purified using the Qiagen RNase-Free DNase set, and then after quantification, the extracted RNA was converted to cDNA using a high capacity RNA-to-cDNA kit from Applied Biosystems (Thermo Fisher Scientific). The levels of AR, TMPRSS2, FKBP5, PSA (KLK3), and GAPDH were quantified using TaqMan Fast Advanced Master Mix from Applied Biosystems. The level of gene expression was evaluated using the

comparative CT method, which compares the CT value to GAPDH (ΔCT) and then to vehicle control ($\Delta\Delta$CT).

Microsomal Metabolic Stability Assay. In vitro microsomal metabolic stability studies of AR degraders were performed in Medicilon Inc (Shanghai, China). The metabolic stability of a test compound was assessed using pooled mouse, rat, dog, monkey, and human liver microsomes, which were purchased from XenoTech (Lenexa, Kansas). Briefly, 1 μM of a test compound was incubated with 0.5 mg/mL of the respective liver microsome and 1.7 mM cofactor-NADPH in 0.1 M K-phosphate buffer (pH = 7.4) containing 5 mM MgCl$_2$ at 37 °C, with the acetonitrile concentration less than 0.1% in the final incubation solution. After 0, 5, 10, 15, 30, and 45 min of incubation, the reaction was stopped immediately by adding 150 μL cold acetonitrile containing IS to each 45 μL incubation solution in the wells of corresponding plates, respectively. The incubation without the addition of NADPH was used as the negative control. Ketanserin was used as the positive control. After quenching, the plate was shaken for 10 min (600 rpm/min), centrifuged at 6000 rpm for 15 min. 80 μL of the supernatant was then transferred from each well into a 96-well plate containing 140 μL of water for LC−MS/MS analysis, from which the remaining amount of the test compound was determined. The natural log of the remaining amount of the test compound was plotted against time to determine the disappearance rate and the half-life of the test compound.

Hepatocyte Stability Assay. Pooled mixed-gender cryopreserved human, monkey, mouse, rat, and dog hepatocytes were obtained from different commercial sources and stored in liquid nitrogen until use. Before experiments, the vial of cryopreserved hepatocytes was removed from the liquid nitrogen storage unit and thawed rapidly in a shaking water bath at 37 °C. The contents of each vial were poured into 40 mL of prewarmed (37 °C) William's Medium E medium (WME, pH 7.4) and gently mixed before centrifugation at 500 rpm for 5 min at room temperature. After centrifugation, the supernatant was discarded without disturbing the cell pellet. The cell is resuspended with preheated WME. Then the hepatocyte cells were counted, and the cell suspension was diluted to the appropriated density (viable cell density = 2 × 10^6 cells/mL). Viabilities for each hepatocyte experiment were at least 80%. The cell suspension was diluted in WME to give two times the incubation concentration and prewarmed at 37 °C for 15 min. 4 mM spiking solution was made by adding 20 μL of substrates stock solution (10 mM) into 30 μL of DMSO. 2 μL of 4 mM spiking solution was added into 3998 μL of WME to make 2× dosing solution (2 μM). To prepare the testing, 40 μL of pre-warmed hepatocytes solution (2 × 10^6 cells/mL) was added to the 48-wells tissue culture-treated polystyrene incubation plate designated for different time-points. Incubations (performed in duplicate) were initiated by the addition of 40 μL prewarmed 2× dosing solution to the wells designed for 5, 15, 30, 60, 120 min, and start timing (1 μM final substrate concentration). The assay plate was placed in an incubator at 37 °C, 5% CO$_2$, and shaken at 110 rpm. For 0 min, 240 μL of ACN containing IS was added to the wells of 0 min plate, followed by addition of 40 μL 2× dosing solution. The plate was then sealed. For other time-points, reactions were terminated at 5, 15, 30, 60, and 120 min by adding 240 μL of ACN containing IS to the wells, respectively. The plate was sealed and stored at a −35 °C freezer. After samples for all the time-points were collected, the plate was shaken for 2 min and then centrifuged at 6000 rpm for 15 min. Finally, 100 μL of the supernatant was transferred from each well into a clean 96-well sample plate containing 100 μL of water for LC/MS analysis.

Plasma Stability Assay. The in vitro plasma stability of a test compound was studied in human, mouse, rat, dog, and monkey plasmas in Medicilon Inc (Shanghai, China). Human plasma was purchased from ZenBio (Durham, NC, USA), and other plasmas were prepared in-house. A test compound was dissolved in DMSO to a final concentration of 10 mM and then diluted to 10 μM in 0.1 M K/Mg-buffer. 90 μL of pre-warmed plasma at 37 °C was added to the wells of a 96-well plate before spiking them with the 10 μL of 10 μM test compound to make the final concentration of the test compound at 1 μM. The spiked plasma samples were incubated at 37 °C for 2 h.

Reactions were terminated at 0, 5, 15, 30, 60, and 120 min by adding 400 μL of acetonitrile containing IS. After quenching, the plates were shaken for 5 min at 600 rpm and stored at −20 °C if necessary, before analysis by LC/MS. Before LC/MS analysis, the samples were thawed at room temperature and centrifuged at 6000 rpm for 20 min. 100 μL of the supernatant from each well was transferred into a 96-well sample plate containing 100 μL of water for LC/MS analysis. Procaine was used as reference control compound for human, mouse, dog, and monkey plasma stability studies, and Benfluorex was used as reference control compound for rat plasma stability studies. The in vitro plasma half-life ($t_{1/2}$) was calculated using the expression $t_{1/2} = 0.693/b$, where b is the slope found in the linear fit of the natural logarithm of the fraction remaining of the test compound vs incubation time.

Plasma Protein Binding Assay. Plasma protein binding of a test compound was assessed by the equilibrium dialysis method with dialysis membrane strips in Medicilon Inc (Shanghai, China). The 96-well equilibrium dialysis plate and dialysis membrane strips were purchased from commercial sources. Pooled human, mouse, rat, dog, and monkey plasmas were used for protein-binding assay on the plasma side and 0.1 M sodium phosphate buffer (pH 7.4) was used on the buffer side. Dialysis membrane strips were soaked in distilled water for an hour, with 20% by volume ethanol added to soak for a further 20 min. The membrane strips were then rinsed in distilled water three times before use. Aliquots of 100 μL of blank dialysis buffer were applied to the receiver side of dialysis chambers. Then, aliquots of 100 μL of the plasma spiked with 1 μM test and reference compounds were applied to the donor side of the dialysis chambers. Warfarin was used as the positive reference control in all plasma protein binding test. The dialysis plate was covered with a plastic lid, and the entire apparatus was placed in a shaker (60 rpm) for 5 h at 37 °C. After 5 h incubation, 25 μL from both the donor sides and receiver sides of the dialysis apparatus were aliquoted into new sample preparation plates and the aliquots were mixed with the same volume of opposite matrixes (blank buffer to plasma and vice versa). Then, the samples with 200 μL acetonitrile containing internal standard (IS) were quenched. Next all the samples were vortexed at 600 rpm for 10 min, followed by centrifugation at 6000 rpm for 15 min. Finally, 100 μL of the supernatant was transferred from each well into a 96-well sample plate containing 100 μL of ultrapure water for LC/MS analysis. The fraction unbound was calculated as % free = (peak area ratio buffer chamber/peak area ratio plasma chamber) × 100%. Analogously, the % bound was calculated as % bound = 100% − % free. Recovery was also evaluated to account for unspecific binding using the equation of % recovery = (peak area ratio buffer chamber + peak area ratio plasma chamber)/peak area ratio initial plasma sample × 100%.

CYP Inhibition Assay. The CYP inhibition of a test compound was studied in human liver microsomes in Medicilon Inc (Shanghai, China). Briefly, 0.2 mg/mL human liver microsome stock solution was prepared by adding 10 μL of 20 mg/mL microsome to 990 μL of 0.1 M KH$_2$PO$_4$ (pH 7.4). In general, human liver microsomes were mixed with buffer (0.1 M K-buffer), a test compound or a reference inhibitor, and warmed to 37 °C in a 96-well temperature-controlled heater block for 5 min. Aliquots of this mixture (30 μL and in duplicate) were delivered to each well of a 96-well polypropylene polymerase chain reaction plate maintained at 37 °C, followed by adjoining of a substrate (15 μL) as applicable. Final organic solvent concentration was 1% (v/v) or less. Incubation was commenced with addition of NADPH stock solution (15 μL, 8 mM, pre-incubated at 37 °C) to a final incubation volume of 60 μL and maintained at 37 °C for a period (5 min for 3A4, 10 min for 1A2, 2B6, and 2C9, 20 min for 2C8 and 2D6, and 45 min for 2C19). Incubations were typically terminated by adding 180 μL of cold CAN-containing IS. After quenching, the plates were shaken at the vibrator for 10 min (600 rpm/min) and then centrifuged at 6000 rpm for 15 min. 80 μL of the supernatant was transferred from each well into a 96-well sample plate containing 120 μL of ultra-pure water for LC/MS analysis. Phenacetin, amfebutamone HCl, paclitaxel, diclofenac, S-mepheny-toin, and dextromethorphan were used as substrates for CYP 1A2,

2B6, 2C8, 2C9, 2C19, and 2D6 isoforms, respectively, and midazolam and testosterone as substrates for CYP 3A4. α-Naphthoflavon, ticlopidine, montelukast, sulfaphenazole, omeprazole, quinidine, and ketoconazole were used as reference inhibitor controls for CYP 1A2, 2B6, 2C8, 2C9, 2C19, 2D6, and 3A4, respectively.

hERG Assay. ARD-2051 was tested for its effect on hERG (human ether-à-go-go-related gene) potassium channels in a HEK 293 cell line stably expressed hERG using the manual patch-clamp technique.[43] Briefly, ARD-2051 was tested at 3 and 30 μM in duplicate, with terfenadine included as the positive control. ARD-2051 or the positive article was tested at room temperature using the whole-cell patch clamp technique[43] with a PatchMaster patch-clamp system (HEKA Elektronik, Germany).

PK Studies in Mice, Rats, and Dogs. PK studies in mice, rats, and dogs were performed in Medicilon, Inc (Shanghai, China). Male ICR mice, male Sprague Dawley (SD) rats, and male beagle dogs were used for PK studies. For mouse PK studies, 10% PEG200 + 90% PBS (adjust pH to 8.0 by 0.5 N NaOH) were used as the formulation both intravenous administration at 2 mg/kg and PO administration at 5 mg/kg. For rat PK studies, 10% PEG400 + 90% PBS (adjust pH to 8.0 by 0.5 N NaOH) were used as the formulation for intravenous administration at 1 mg/kg, and 5% DMSO +10% solutol + 85% saline were used as the formulation for PO administration at 10 mg/kg. For dog PK studies of ARD-2051, 10% PEG400 + 90% PBS (adjust pH to 8.0 by 0.5 N NaOH) as the formulation were used for intravenous administration at 1 mg/kg and 90% PEG400 + 10% cremophor as the formulation were used for PO administration at 3 mg/kg.

Animals were dosed with testing compound ARD-2051 in its respective formulations, followed by collection of blood samples (100−200 μL) from individual cohorts of animal (n = 3) using heparinized calibrated pipettes or tubes (at 5 min, 15 min, 30 min, 1 h, 2 h, 4 h, 6 h, 8 h, and 24 h), and centrifuged at 6800g for 6 min at 2−8 °C. Subsequently, the resulting plasma was transferred to appropriately labeled tubes within 1 h of blood collection/ centrifugation and stored frozen at −80 °C for analysis.

An aliquot of 20 μL plasma from each sample was protein precipitated with 400 μL MEOH, which contains 100 ng/mL IS. The mixture was vortexed for 1 min and centrifuged at 18,000g for 10 min. Then 200 μL of supernatant was transferred to 96-well plates for LC−MS/MS analysis. To determine drug concentrations in plasma, a LC−MS/MS method was developed and validated for ARD-2051. The LC−MS/MS method consisted of an UPLC system, and chromatographic separation of ARD-2051 was achieved using a Waters ACQUITY UPLC BEH C18 1.7 μm column (2.1*50 mm). A Sciex QTrap 6500+ mass spectrometer equipped with an electrospray ionization source (Applied biosystems, Toronto, Canada) in the positive-ion multiple reaction monitoring (MRM) mode was used for detection. The precursor/product ion transitions were monitored at m/z 789.40−392.30, and 271.10−172.00 for ARD-2051 and IS tolbutamide, respectively, in the positive electrospray ionization mode. The mobile phases used on UPLC were 0.1% formic acid in purified water (A) and 0.1% formic acid in acetonitrile (B). The gradient (B) was held at 10% (0−0.1 min), increased to 90% at 0.7 min, then maintained at isocratic 90% B for 0.4 min, and then immediately stepped back down to 10% for 0.3 min re-equilibration. The flow rate was set at 0.6 mL/min. A column oven was set at 40 °C. An aliquot of 1 μL supernatant was injected for LC−MS/MS analysis using an autosampler. The analytical results were confirmed using quality control samples for intra-assay variation. The accuracy of >66.7% of the quality control samples was between 80 and 120% of the known value(s). All PK parameters were calculated by noncompartmental methods using Phoenix WinNonlin, version 7.0 (Pharsight, USA).

PK/PD and Efficacy Studies in Mice. With the exception of PK studies in mice, rats, and dogs, all other in vivo studies were performed under animal protocols (PRO00011174 and PRO00009463) approved by the Institutional Animal Care & Use Committee (IACUC) of the University of Michigan, in accordance with the recommendations in the Guide for the Care and Use of Laboratory Animals of the National Institutes of Health.

To grow VCaP xenograft tumors, male CB17 SCID mice (Charles River Laboratories) were injected subcutaneously with 5×10^6 VCaP cells (ATCC) in 5 mg/mL Matrigel (Corning).

For determination of oral exposures for AR degraders, each compound was administered in non-tumor-bearing male mice via oral gavage using 100% PEG200 as the dosing vehicle. Animals were sacrificed at indicated time-points with 3 mice for each time-point for each compound, and 300 μL of blood was collected from each animal and were stored at −80 °C until analysis.

For PK/PD studies in tumor-bearing male SCID mice, each compound was administered in animals via oral gavage using 100% PEG200 as the dosing vehicle when the VCaP tumors reached approximately 200 mm³. Animals were sacrificed at indicated time-points with 3 mice for each compound at each time-point, and blood (300 μL) and tumor were collected from each animal for analysis. Isolated tumor samples were immediately frozen and ground with a mortar and pestle in liquid nitrogen. All plasma and tumor samples were stored at −80 °C until analysis. For analysis of AR protein levels in tumor samples, resected VCaP xenograft tumor tissues were ground into powder in liquid nitrogen and lysed in CST lysis buffer with halt proteinase inhibitors. 20 μg of whole tumor clarified lysates was separated on 4−20 or 4−12% Novex gels. Western blots were performed as detailed in the previous section.

All PK/PD and efficacy animal experiments in this study were approved by the University of Michigan Committee on Use and Care of Animals and Unit for Laboratory Animal Medicine (ULAM). The PKs of ARD-2051 and analogs were determined in tumor-free female SCID mice or with VCAP tumor following oral gavage (PO) single dose at 10 or 20 mg/kg. The solid compounds were dissolved in a vehicle containing 100% PEG200. The animals (total 9 mice/ compound or 6 mice/compound) were sacrificed at 1, 3, and 6 h or 6 and 24 h after final administration of the chemicals, followed by collection of blood samples (300 μL) and tumor samples. The blood samples were centrifuged at 15,000 rpm for 10 min, and then the supernatant plasma was saved for analysis. Isolated tumor samples were immediately frozen and ground with a mortar and pestle in liquid nitrogen. All plasma and tumor samples were stored at −80 °C until analysis. To prepare tumor samples for LCMS analysis, mixed ultrapure water and acetonitrile solution (4:1) were added to the defrosted tumor tissue samples 5:1, v/w, in order to facilitate homogenization with Precellys evolution homogenizer under 4 °C. The homogenized tissue solution was denatured using cold acetonitrile (1:3, v/v) with vortex and centrifuged at 13,000 rpm 4 °C for 10 min. Following protein precipitation, the final supernatants were collected for LCMS analysis.

To determine drug concentrations in plasma and tumor samples, an LC−MS/MS method was developed and validated. The LC−MS/ MS method consisted of a Shimadzu HPLC system, and chromatographic separation of a test compound was achieved using a Waters XBridge-C18 column (5 cm × 2.1 mm, 3.5 μm). An AB Sciex QTrap 5500 mass spectrometer equipped with an electrospray ionization source (Applied biosystems, Toronto, Canada) in the positive-ion MRM mode was used for detection. For example, the precursor/ product ion transitions were monitored at m/z 820.3−542.2 and 455.2−425.2 for ARD-2051 and IS, respectively, in the positive electrospray ionization mode. The mobile phases used on HPLC were 0.1% formic acid in purified water (A) and 0.1% formic acid in acetonitrile (B). The gradient (B) was held at 10% (0−0.3 min), increased to 95% at 0.7 min, then maintained at isocratic 95% B for 2.3 min, and then immediately stepped back down to 10% for 2 min re-equilibration. The flow rate was set at 0.4 mL/min. All PK parameters were calculated by noncompartmental methods using WinNonlin, version 3.2 (Pharsight Corporation, Mountain View, CA, USA).

For the in vivo efficacy experiments, when VCaP tumors reached an average volume of 150 mm³, mice were tumor size-matched and randomly assigned to different experimental groups with 7 mice for each group. Drugs or vehicle control were given at the dose schedule as indicated using 100% PEG200 as the dosing vehicle. Tumor sizes and animal weights were measured 2−3 times per week. Tumor

volume (mm^3) = (length × width^2)/2. Tumor growth inhibition was calculated as TGI (%) = (Vc − Vt)/(Vc − Vo)*100, where Vc and Vt are the medians of the control and treated groups at the end of the treatment, respectively, and Vo is that at the start. Tumor volumes at the end of treatment were statistically analyzed using a two-tailed, unpaired t-test (GraphPad Prism 8,0).

■ ASSOCIATED CONTENT

ⓢ Supporting Information

The Supporting Information is available free of charge at https://pubs.acs.org/doi/10.1021/acs.jmedchem.3c00405.

> ^{1}H and ^{13}C NMR spectra for representative AR degraders and HPLC purity spectra for representative AR degraders (PDF)
>
> Predicted binding models for ligands **14a** (PDB)
>
> Predicted binding models for ligands **15a** (PDB)
>
> Molecular string file for all the final target compounds (CSV)

■ AUTHOR INFORMATION

Corresponding Author

> **Shaomeng Wang** − *The Rogel Cancer Center, University of Michigan, Ann Arbor, Michigan 48109, United States; Department of Internal Medicine, Department of Pharmacology, and Department of Medicinal Chemistry, University of Michigan, Ann Arbor, Michigan 48109, United States;* ⓞ orcid.org/0000-0002-8782-6950; Email: Shaomeng@umich.edu

Authors

> **Xin Han** − *The Rogel Cancer Center, University of Michigan, Ann Arbor, Michigan 48109, United States; Department of Internal Medicine, University of Michigan, Ann Arbor, Michigan 48109, United States; Present Address: Cancer Institute (Key Laboratory of Cancer Prevention and Intervention, China National Ministry of Education) of the 2nd Affiliated Hospital and Institute of Translational Medicine, Zhejiang University School of Medicine, Hangzhou 310029, China;* ⓞ orcid.org/0000-0003-0904-220X
>
> **Lijie Zhao** − *The Rogel Cancer Center, University of Michigan, Ann Arbor, Michigan 48109, United States; Department of Internal Medicine, University of Michigan, Ann Arbor, Michigan 48109, United States*
>
> **Weiguo Xiang** − *The Rogel Cancer Center, University of Michigan, Ann Arbor, Michigan 48109, United States; Department of Internal Medicine, University of Michigan, Ann Arbor, Michigan 48109, United States*
>
> **Bukeyan Miao** − *The Rogel Cancer Center, University of Michigan, Ann Arbor, Michigan 48109, United States; Department of Internal Medicine, University of Michigan, Ann Arbor, Michigan 48109, United States*
>
> **Chong Qin** − *The Rogel Cancer Center, University of Michigan, Ann Arbor, Michigan 48109, United States; Department of Internal Medicine, University of Michigan, Ann Arbor, Michigan 48109, United States; Present Address: Key Laboratory of Marine Drugs, Chinese Ministry of Education, School of Medicine and Pharmacy, Ocean University of China, Qingdao, Shandong 266003, China; Center for Targeted Protein Degradation and Drug Discovery, Ocean University of China, Qingdao, Shandong 266003, China; Laboratory for Marine Drugs and Bioproducts, Pilot National Laboratory for Marine Science and Technology, Qingdao, Shandong 266137, China;* ⓞ orcid.org/0000-0001-8108-1698
>
> **Mi Wang** − *The Rogel Cancer Center, University of Michigan, Ann Arbor, Michigan 48109, United States; Department of Internal Medicine, University of Michigan, Ann Arbor, Michigan 48109, United States*
>
> **Tianfeng Xu** − *The Rogel Cancer Center, University of Michigan, Ann Arbor, Michigan 48109, United States; Department of Internal Medicine, University of Michigan, Ann Arbor, Michigan 48109, United States; Present Address: Department of Medicinal Chemistry, Shanghai Institute of Materia Medica, Chinese Academy of Sciences, Shanghai 201203, China; University of Chinese Academy of Sciences, Beijing 100049, China; School of Pharmaceutical Science and Technology, Hangzhou Institute for Advanced Study, University of Chinese Academy of Sciences, Hangzhou 310024, China;* ⓞ orcid.org/0000-0001-8996-4065
>
> **Donna McEachern** − *The Rogel Cancer Center, University of Michigan, Ann Arbor, Michigan 48109, United States; Department of Internal Medicine, University of Michigan, Ann Arbor, Michigan 48109, United States*
>
> **Jianfeng Lu** − *The Rogel Cancer Center, University of Michigan, Ann Arbor, Michigan 48109, United States; Department of Internal Medicine, University of Michigan, Ann Arbor, Michigan 48109, United States*
>
> **Yu Wang** − *The Rogel Cancer Center, University of Michigan, Ann Arbor, Michigan 48109, United States; Department of Internal Medicine, University of Michigan, Ann Arbor, Michigan 48109, United States*
>
> **Hoda Metwally** − *The Rogel Cancer Center, University of Michigan, Ann Arbor, Michigan 48109, United States; Department of Internal Medicine, University of Michigan, Ann Arbor, Michigan 48109, United States*
>
> **Chao-Yie Yang** − *The Rogel Cancer Center, University of Michigan, Ann Arbor, Michigan 48109, United States; Department of Internal Medicine, University of Michigan, Ann Arbor, Michigan 48109, United States; Present Address: Departments of Pharmaceutical Sciences, College of Pharmacy, University of Tennessee Health Science Center, Memphis, Tennessee 38163, United States;* ⓞ orcid.org/0000-0002-5445-0109
>
> **Paul D. Kirchhoff** − *The Rogel Cancer Center, University of Michigan, Ann Arbor, Michigan 48109, United States; Department of Internal Medicine, University of Michigan, Ann Arbor, Michigan 48109, United States*
>
> **Lu Wang** − *Department of Pharmaceutical Sciences, College of Pharmacy, University of Michigan, Ann Arbor, Michigan 48109, United States*
>
> **Aleksas Matvekas** − *Department of Pharmaceutical Sciences, College of Pharmacy, University of Michigan, Ann Arbor, Michigan 48109, United States*
>
> **John Takyi-Williams** − *Department of Pharmaceutical Sciences, College of Pharmacy, University of Michigan, Ann Arbor, Michigan 48109, United States*
>
> **Bo Wen** − *Department of Pharmaceutical Sciences, College of Pharmacy, University of Michigan, Ann Arbor, Michigan 48109, United States*
>
> **Duxin Sun** − *Department of Pharmaceutical Sciences, College of Pharmacy, University of Michigan, Ann Arbor, Michigan 48109, United States;* ⓞ orcid.org/0000-0002-6406-2126
>
> **Mark Ator** − *Oncopia Therapeutics Inc, Malvern, Pennsylvania 19355, United States*

Robert Mckean − *Oncopia Therapeutics Inc, Malvern, Pennsylvania 19355, United States*

Complete contact information is available at:
https://pubs.acs.org/10.1021/acs.jmedchem.3c00405

Author Contributions

[¶]X.H., L.Z., W.X., B. M., C. Q., and M.W. contributed equally.

Notes

The authors declare the following competing financial interest(s): The University of Michigan has filed patent applications on these AR degraders, which have been licensed to Oncopia Therapeutics, Inc. S. Wang, X. Han, W. Xiang, L. Zhao, B. Miao, C. Qin, T. Xu, C.-Y. Yang, and J. Lu are co-inventors on one or more of these patent applications and receive royalties from the University of Michigan. S. Wang was a co-founder of Oncopia Therapeutics and a paid consultant to Oncopia Therapeutics. S. Wang and the University of Michigan also owned equity in Oncopia, which was acquired by Roivant Sciences. S. Wang is a paid consultant to Roivant Sciences and Proteovant Therapeutics and owns equity in Roivant Sciences. The University of Michigan has received a research contract from Proteovant Therapeutics, Inc. and Oncopia Therapeutics (acquired by Roivant Sciences) for which S. Wang serves as the principal investigator.

◼ ABBREVIATIONS USED

PCa, prostate cancer; AR, androgen receptor; ADT, androgen deprivation therapy; mCRPC, metastatic castration-resistant prostate cancer; PROTAC, proteolysis targeting chimera; SNIPERs, specific and nongenetic IAP-dependent protein erasers; PK, pharmacokinetics; V_{ss}, steady-state volume of distribution; C_{max}, maximum drug concentration; AUC_{0-24h}, area-under-the-curve between 0 and 24 h; Cl, plasma clearance rate; $T_{1/2}$, terminal half-life; F, oral bioavailability; IV, intravenous administration; PO, oral administration; SD, standard deviation; PD, pharmacodynamics; CYP, cytochrome P450; TMS, tetramethylsilane; MS, mass spectrometric; ATCC, american type culture collection; qRT-PCR, quantitative real-time polymerase chain reaction; IACUC, Institutional Animal Care & Use Committee; SCID, severe combined immunodeficient; ULAM, Unit for Laboratory Animal Medicine; MRM, multiple reaction monitoring

◼ REFERENCES

(1) Rebello, R. J.; Oing, C.; Knudsen, K. E.; Loeb, S.; Johnson, D. C.; Reiter, R. E.; Gillessen, S.; Van der Kwast, T.; Bristow, R. G. Prostate cancer. *Nat. Rev. Dis. Primers* **2021**, 7, 9.

(2) Elmehrath, A. O.; Afifi, A. M.; Al-Husseini, M. J.; Saad, A. M.; Wilson, N.; Shohdy, K. S.; Pilie, P.; Sonbol, M. B.; Alhalabi, O. Causes of Death Among Patients With Metastatic Prostate Cancer in the US From 2000 to 2016. *JAMA Netw. Open* **2021**, 4, No. e2119568.

(3) Fujita, K.; Nonomura, N. Role of Androgen Receptor in Prostate Cancer: A Review. *World J. Men's Health* **2019**, 37, 288−295.

(4) Sawant, M.; Mahajan, K.; Renganathan, A.; Weimholt, C.; Luo, J.; Kukshal, V.; Jez, J. M.; Jeon, M. S.; Zhang, B.; Li, T.; Fang, B.; Luo, Y.; Lawrence, N. J.; Lawrence, H. R.; Feng, F. Y.; Mahajan, N. P.

Chronologically modified androgen receptor in recurrent castration-resistant prostate cancer and its therapeutic targeting. *Sci. Transl. Med.* **2022**, 14, No. eabg4132.

(5) Crawford, E. D.; Heidenreich, A.; Lawrentschuk, N.; Tombal, B.; Pompeo, A. C. L.; Mendoza-Valdes, A.; Miller, K.; Debruyne, F. M. J.; Klotz, L. Androgen-targeted therapy in men with prostate cancer: evolving practice and future considerations. *Prostate Cancer Prostatic Dis.* **2019**, 22, 24−38.

(6) Perera, M.; Roberts, M. J.; Klotz, L.; Higano, C. S.; Papa, N.; Sengupta, S.; Bolton, D.; Lawrentschuk, N. Intermittent versus continuous androgen deprivation therapy for advanced prostate cancer. *Nat. Rev. Urol.* **2020**, 17, 469−481.

(7) Higano, C. Enzalutamide, apalutamide, or darolutamide: are apples or bananas best for patients? *Nat. Rev. Urol.* **2019**, 16, 335−336.

(8) Al-Salama, Z. T. Apalutamide: A Review in Non-Metastatic Castration-Resistant Prostate Cancer. *Drugs* **2019**, 79, 1591−1598.

(9) Mori, K.; Mostafaei, H.; Pradere, B.; Motlagh, R. S.; Quhal, F.; Laukhtina, E.; Schuettfort, V. M.; Abufaraj, M.; Karakiewicz, P. I.; Kimura, T.; Egawa, S.; Shariat, S. F. Apalutamide, enzalutamide, and darolutamide for non-metastatic castration-resistant prostate cancer: a systematic review and network meta-analysis. *Int. J. Clin. Oncol.* **2020**, 25, 1892−1900.

(10) Verma, S.; Prajapati, K. S.; Kushwaha, P. P.; Shuaib, M.; Singh, A. K.; Kumar, S.; Gupta, S. Resistance to second generation antiandrogens in prostate cancer: pathways and mechanisms. *Cancer Drug Resist.* **2020**, 3, 742−761.

(11) Rice, M. A.; Malhotra, S. V.; Stoyanova, T. Second-Generation Antiandrogens: From Discovery to Standard of Care in Castration Resistant Prostate Cancer. *Front. Oncol.* **2019**, 9, 801.

(12) Orme, J. J.; Pagliaro, L. C.; Quevedo, J. F.; Park, S. S.; Costello, B. A. Rational Second-Generation Antiandrogen Use in Prostate Cancer. *Oncologist* **2022**, 27, 110−124.

(13) Watson, P. A.; Arora, V. K.; Sawyers, C. L. Emerging mechanisms of resistance to androgen receptor inhibitors in prostate cancer. *Nat. Rev. Cancer* **2015**, 15, 701−711.

(14) Jernberg, E.; Bergh, A.; Wikström, P. Clinical relevance of androgen receptor alterations in prostate cancer. *Endocr. Connect.* **2017**, 6, R146−R161.

(15) Rana, M.; Dong, J.; Robertson, M. J.; Basil, P.; Coarfa, C.; Weigel, N. L. Androgen receptor and its splice variant, AR-V7, differentially induce mRNA splicing in prostate cancer cells. *Sci. Rep.* **2021**, 11, 1393.

(16) Morova, T.; McNeill, D. R.; Lallous, N.; Gönen, M.; Dalal, K.; Wilson, D. M.; Gürsoy, A.; Keskin, Ö.; Lack, N. A. Androgen receptor-binding sites are highly mutated in prostate cancer. *Nat. Commun.* **2020**, 11, 832.

(17) Makino, T.; Izumi, K.; Mizokami, A. Undesirable Status of Prostate Cancer Cells after Intensive Inhibition of AR Signaling: Post-AR Era of CRPC Treatment. *Biomedicines* **2021**, 9, 414.

(18) Xiang, W.; Wang, S. Therapeutic Strategies to Target the Androgen Receptor. *J. Med. Chem.* **2022**, 65, 8772−8797.

(19) Sakamoto, K. M.; Kim, K. B.; Kumagai, A.; Mercurio, F.; Crews, C. M.; Deshaies, R. J. Protacs: Chimeric molecules that target proteins to the Skp1-Cullin-F box complex for ubiquitination and degradation. *P Natl Acad Sci USA* **2001**, 98, 8554−8559.

(20) Lai, A. C.; Crews, C. M. Induced protein degradation: an emerging drug discovery paradigm. *Nat. Rev. Drug Discovery* **2017**, 16, 101−114.

(21) Schneekloth, A. R.; Pucheault, M.; Tae, H. S.; Crews, C. M. Targeted intracellular protein degradation induced by a small molecule: En route to chemical proteomics. *Bioorg. Med. Chem. Lett.* **2008**, 18, 5904−5908.

(22) Ito, T.; Ando, H.; Suzuki, T.; Ogura, T.; Hotta, K.; Imamura, Y.; Yamaguchi, Y.; Handa, H. Identification of a Primary Target of Thalidomide Teratogenicity. *Science* **2010**, 327, 1345−1350.

(23) Sekine, K.; Takubo, K.; Kikuchi, R.; Nishimoto, M.; Kitagawa, M.; Abe, F.; Nishikawa, K.; Tsuruo, T.; Naito, M. Small molecules

destabilize cIAP1 by activating auto-ubiquitylation. *J. Biol. Chem.* **2008**, *283*, 8961−8968.

(24) Itoh, Y.; Ishikawa, M.; Naito, M.; Hashimoto, Y. Protein Knockdown Using Methyl Bestatin-Ligand Hybrid Molecules: Design and Synthesis of Inducers of Ubiquitination-Mediated Degradation of Cellular Retinoic Acid-Binding Proteins. *J. Am. Chem. Soc.* **2010**, *132*, 5820−5826.

(25) Kronke, J.; Udeshi, N. D.; Narla, A.; Grauman, P.; Hurst, S. N.; McConkey, M.; Svinkina, T.; Heckl, D.; Comer, E.; Li, X. Y.; Ciarlo, C.; Hartman, E.; Munshi, N.; Schenone, M.; Schreiber, S. L.; Carr, S. A.; Ebert, B. L. Lenalidomide Causes Selective Degradation of IKZF1 and IKZF3 in Multiple Myeloma Cells. *Science* **2014**, *343*, 301−305.

(26) Kronke, J.; Fink, E. C.; Hollenbach, P. W.; MacBeth, K. J.; Hurst, S. N.; Udeshi, N. D.; Chamberlain, P. P.; Mani, D. R.; Man, H. W.; Gandhi, A. K.; Svinkina, T.; Schneider, R. K.; McConkey, M.; Jaras, M.; Griffiths, E.; Wetzler, M.; Bullinger, L.; Cathers, B. E.; Carr, S. A.; Chopra, R.; Ebert, B. L. Lenalidomide induces ubiquitination and degradation of CK1α in del(5q) MDS. *Nature* **2015**, *523*, 183−188.

(27) Shibata, N.; Nagai, K.; Morita, Y.; Ujikawa, O.; Ohoka, N.; Hattori, T.; Koyama, R.; Sano, O.; Imaeda, Y.; Nara, H.; Cho, N.; Naito, M. Development of Protein Degradation Inducers of Androgen Receptor by Conjugation of Androgen Receptor Ligands and Inhibitor of Apoptosis Protein Ligands. *J. Med. Chem.* **2018**, *61*, 543−575.

(28) Salami, J.; Alabi, S.; Willard, R. R.; Vitale, N. J.; Wang, J.; Dong, H.; Jin, M.; McDonnell, D. P.; Crew, A. P.; Neklesa, T. K.; Crews, C. M. Androgen receptor degradation by the proteolysis-targeting chimera ARCC-4 outperforms enzalutamide in cellular models of prostate cancer drug resistance. *Commun. Biol.* **2018**, *1*, 100.

(29) Han, X.; Wang, C.; Qin, C.; Xiang, W.; Fernandez-Salas, E.; Yang, C.-Y.; Wang, M.; Zhao, L.; Xu, T.; Chinnaswamy, K.; Delproposto, J.; Stuckey, J.; Wang, S. Discovery of ARD-69 as a Highly Potent Proteolysis Targeting Chimera (PROTAC) Degrader of Androgen Receptor (AR) for the Treatment of Prostate Cancer. *J. Med. Chem.* **2019**, *62*, 941−964.

(30) Han, X.; Zhao, L.; Xiang, W.; Qin, C.; Miao, B.; Xu, T.; Wang, M.; Yang, C. Y.; Chinnaswamy, K.; Stuckey, J.; Wang, S. Discovery of Highly Potent and Efficient PROTAC Degraders of Androgen Receptor (AR) by Employing Weak Binding Affinity VHL E3 Ligase Ligands. *J. Med. Chem.* **2019**, *62*, 11218−11231.

(31) Jimenez, D. G.; Sebastiano, M. R.; Caron, G.; Ermondi, G. Are we ready to design oral PROTACs? *ADMET DMPK* **2021**, *9*, 243−254.

(32) Gao, X.; Burris, H. A., III; Vuky, J.; Dreicer, R.; Sartor, A. O.; Sternberg, C. N.; Percent, I. J.; Hussain, M. H. A.; Rezazadeh Kalebasty, A.; Shen, J.; Heath, E. I.; Abesada-Terk, G.; Gandhi, S. G.; McKean, M.; Lu, H.; Berghorn, E.; Gedrich, R.; Chirnomas, S. D.; Vogelzang, N. J.; et al. Phase 1/2 study of ARV-110, an androgen receptor (AR) PROTAC degrader, in metastatic castration-resistant prostate cancer (mCRPC). *J. Clin. Oncol.* **2022**, *40*, 17.

(33) Han, X.; Zhao, L.; Xiang, W.; Qin, C.; Miao, B.; McEachern, D.; Wang, Y.; Metwally, H.; Wang, L.; Matvekas, A.; Wen, B.; Sun, D.; Wang, S. Strategies toward Discovery of Potent and Orally Bioavailable Proteolysis Targeting Chimera Degraders of Androgen Receptor for the Treatment of Prostate Cancer. *J. Med. Chem.* **2021**, *64*, 12831−12854.

(34) Xiang, W.; Zhao, L.; Han, X.; Qin, C.; Miao, B.; McEachern, D.; Wang, Y.; Metwally, H.; Kirchhoff, P. D.; Wang, L.; Matvekas, A.; He, M.; Wen, B.; Sun, D.; Wang, S. Discovery of ARD-2585 as an Exceptionally Potent and Orally Active PROTAC Degrader of Androgen Receptor for the Treatment of Advanced Prostate Cancer. *J. Med. Chem.* **2021**, *64*, 13487−13509.

(35) Inuzuka, H.; Liu, J.; Wei, W.; Rezaeian, A. H. PROTACs technology for treatment of Alzheimer's disease: Advances and perspectives. *Acta Mater. Med.* **2022**, *1*, 24−41.

(36) Han, X.; Wei, W.; Sun, Y. PROTAC Degraders with Ligands Recruiting MDM2 E3 Ubiquitin Ligase: An Updated Perspective. *Acta Mater. Med.* **2022**, *1*, 244−259.

(37) Han, X.; Sun, Y. Strategies for the discovery of oral PROTAC degraders aimed at cancer therapy. *Cell Rep. Phys. Sci.* **2022**, *3*, 101062.

(38) Bai, L.; Zhou, B.; Yang, C. Y.; Ji, J.; McEachern, D.; Przybranowski, S.; Jiang, H.; Hu, J.; Xu, F.; Zhao, Y.; Liu, L.; Fernandez-Salas, E.; Xu, J.; Dou, Y.; Wen, B.; Sun, D.; Meagher, J.; Stuckey, J.; Hayes, D. F.; Li, S.; Ellis, M. J.; Wang, S. Targeted Degradation of BET Proteins in Triple-Negative Breast Cancer. *Cancer Res.* **2017**, *77*, 2476−2487.

(39) Qin, C.; Hu, Y.; Zhou, B.; Fernandez-Salas, E.; Yang, C. Y.; Liu, L.; McEachern, D.; Przybranowski, S.; Wang, M.; Stuckey, J.; Meagher, J.; Bai, L.; Chen, Z.; Lin, M.; Yang, J.; Ziazadeh, D. N.; Xu, F.; Hu, J.; Xiang, W.; Huang, L.; Li, S.; Wen, B.; Sun, D.; Wang, S. Discovery of QCA570 as an Exceptionally Potent and Efficacious Proteolysis Targeting Chimera (PROTAC) Degrader of the Bromodomain and Extra-Terminal (BET) Proteins Capable of Inducing Complete and Durable Tumor Regression. *J. Med. Chem.* **2018**, *61*, 6685−6704.

(40) Bai, L.; Zhou, H.; Xu, R.; Zhao, Y.; Chinnaswamy, K.; McEachern, D.; Chen, J.; Yang, C. Y.; Liu, Z.; Wang, M.; Liu, L.; Jiang, H.; Wen, B.; Kumar, P.; Meagher, J. L.; Sun, D.; Stuckey, J. A.; Wang, S. A Potent and Selective Small-Molecule Degrader of STAT3 Achieves Complete Tumor Regression In Vivo. *Cancer Cell* **2019**, *36*, 498−511.

(41) *Molecular Operating Environment (MOE)*; Chemical Computing Group ULC, 1010 Sherbrooke St. West, Suite #910: Montreal, QC, Canada, H3A 2R7, 2020.

(42) Case, D. A.; Darden, T. A.; Cheatham, T. E.; Simmerling, C. L.; Wang, J.; Duke, R. E.; Luo, R.; Crowley, M.; Walker, R. C.; Zhang, W.; Merz, K. M.; Wang, B.; Hayik, S.; Roitberg, A.; Seabra, G.; Kolossvary, I.; Wong, K. F.; Paesani, F.; Vanicek, J.; Wu, X.; Brozell, S. R.; Steinbrecher, T.; Gohlke, H.; Yang, L.; Tan, C.; Mongan, J.; Hornak, V.; Cui, G.; Mathews, D. H.; Seetin, M. G.; Sagui, C.; Babin, V.; Kollman, P. A. *Amber 10*; University of California: San Francisco, 2008.

(43) Chen, X. L.; Kang, J. S.; Rampe, D. Manual Whole-Cell Patch-Clamping of the HERG Cardiac K+ Channel. *Methods Mol. Biol.* **2011**, *691*, 151−163.